Assessment of the anti-inflammatory activity of potentially bioactive compounds by intravital microcirculatory analysis

Gabriella Varga

Ph.D. Thesis

Institute of Surgical Research,

University of Szeged

2013

LIST OF PAPERS RELATING TO THE SUBJECT OF THE THESIS

List of full papers relating to the subject of the thesis

1. **VARGA G**, ÉRCES D, FAZEKAS B, FÜLÖP M, KOVÁCS T, KASZAKI J, FÜLÖP F, VÉCSEI L, BOROS M: N-Methyl-D-aspartate receptor antagonism decreases motility and inflammatory activation in the early phase of acute experimental colitis in the rat. *Neurogastroenterol Motil* 2010; 22: 217-225. **IF=3.349**
2. KASZAKI J, ÉRCES D, **VARGA G**, SZABÓ A, VÉCSEI L., BOROS M: Kynurenines and intestinal neurotransmission: the role of N-methyl-D-aspartate receptors. *J Neural Transm* 2012; 119: 211-223. **IF=2.730**
3. KOVÁCS T, **VARGA G**, ÉRCES D, TŐKÉS T, TISZLAVICZ L, GHYCZY M, BOROS M, KASZAKI J: Dietary phosphatidylcholine supplementation attenuates inflammatory mucosal damage in a rat model of experimental colitis. *Shock* 2012; 38: 177-185. **IF=3.203**
4. ÉRCES D, **VARGA G**, FAZEKAS B, KOVÁCS T, TŐKÉS T, TISZLAVICZ L, FÜLÖP F, VÉCSEI L, BOROS M, KASZAKI J: N-Methyl-D-aspartate receptor antagonist therapy suppresses colon motility and inflammatory activation six days after the onset of experimental colitis in rats. *Eur J Pharmacol* 2012; 691: 225-234. **IF=2.737**
5. KOVÁCS T, **VARGA G**, ÉRCES D, TŐKÉS T, TISZLAVICZ L, GHYCZY M, BOROS M, KASZAKI J**:** Terápiás lehetőségek összehasonlító vizsgálata a gyulladásos bélbetegség állatkísérletes modelljében. *Magyar Sebészet* 2012; 65(4): 191-197. **IF=0**

List of abstracts relating to the subject of the thesis

1. ÉRCES D, **VARGA G**, KOVÁCS T, KASZAKI J, VÉCSEI L, BOROS M: Glutamate receptor inhibition improves intestinal function in experimental colitis. *British Journal of Surgery* 2008; 95 (S6): 17.
2. KOVÁCS T, FAZEKAS B, **VARGA G**, ÉRCES D, KASZAKI J, VÉCSEI L, BOROS M: Az NMDA-receptorgátlás vizsgálata bélgyulladásos patkánymodellben. *Magyar Sebészet* 2009; 62: 154.
3. **VARGA G**, KOVÁCS T, KASZAKI J, GHYCZY M, BOROS M: A foszfatidil-etanolamin gyulladáscsökkentő hatása kísérletes colitis modellben. *Magyar Sebészet* 2009; 62: 145-146.
4. FAZEKAS B, **VARGA G**, ÉRCES D, KOVÁCS T, KASZAKI J, VÉCSEI L, BOROS M: Az NMDA-receptor-aktiváció jelentősége kísérletes bélgyulladásban. *Magyar Sebészet* 2009; 62: 153.
5. **VARGA G**, ÉRCES D, FAZEKAS B, FÜLÖP M, KOVÁCS T, KASZAKI J, FÜLÖP F, VÉCSEI L, BOROS M: N-methyl-D-aspartate receptor inhibition decreases motility and inflammatory activation in experimental colitis. *Shock* 2009; 32 (S1): 14.
6. **VARGA G**, ÉRCES D, FAZEKAS B, FÜLÖP M, KOVÁCS T, KASZAKI J, FÜLÖP F, VÉCSEI L, BOROS M: N-methyl-D-aspartate receptor inhibition decreases motility and inflammatory activation in experimental colitis. *Shock* 2009; 32. (Suppl. 1): P18.
7. **VARGA G**, KOVÁCS T, TŐKÉS T, ÉRCES D, KASZAKI J, GHYCZY M, BOROS M: Effects of oral phosphatidylcholine on the inflammatory activation in early and late phases of experimental colitis. *Acta Physiologica* 2011; 202 (S684): 124-125.

OTHER PAPERS RELATING TO THE FIELD OF THE THESIS

1. BOROS M, GHYCZY M, ÉRCES D, **VARGA G**, TŐKÉS T, KUPAI K., TORDAY C, KASZAKI J: The anti-inflammatory effects of methane. *Critical Care Med* 2012; 40(4): 1269-1278. **IF 6.254**

2. **VARGA G**, ÉRCES D, KASZAKI J, GHYCZY M, BOROS M: Metán belélegzés gyulladáscsökkentő hatásának vizsgálata iszkémia-reperfúzió alatt. *Magyar Sebészet* 2012; 65(4): 205-211. **IF=0**

Contents

CLSEM	confocal laser scanning endomicroscopy
CNS	central nervous system
CO	cardiac output
eNOS	endothelial NOS
ENS	enteric nervous system
ET-1	endothelin-1
FCD	functional capillary density
FITC-dextran	fluorescein isothiocyanate-dextran
GI	gastrointestinal
HR	heart rate
IBD	inflammatory bowel disease
IL-6	interleukin-6
iNOS	inducible NOS
IVM	intravital microscopy
KynA	kynurenic acid
MAP	mean arterial pressure
MPO	myeloperoxidase
NMDA	N-methyl-D-aspartate
nNOS	neuronal NOS
NO	nitric oxide
NOS	nitric oxide synthase
NO_x	nitrite/nitrate
OPS	orthogonal polarization spectral imaging technique
PC	phosphatidylcholine
PMN	polymorphonuclear granulocyte
RBCV	red blood cell velocity
ROS	reactive oxygen species
SOX	superoxide
TNBS	trinitrobenzenesulfonic acid
TNF-α	tumor necrosis factor-alpha
TPR	total peripheral resistance
XOR	xanthine oxidoreductase

SUMMARY

Inflammatory reactions play critical roles in determining the survival or destruction of tissues after various injuries. The microvascular system is a decisive mediator of these events, but the microcirculatory aspects of anti-inflammatory therapeutic approaches are rarely investigated. We set out to examine and determine the microcirculatory effects of novel, potentially vasoactive medications with possible anti-inflammatory properties in the gastrointestinal tract. The microcirculatory changes were observed *in vivo* by means of orthogonal polarization spectral imaging technique and confocal laser scanning endomicroscopy in inflammatory models of human gastrointestinal pathologies. The microvascular actions of N-methyl-D-aspartate (NMDA) receptor antagonist compounds and phosphatidylcholine (PC) treatments against the consequences of microcirculatory inflammation, were characterized by detecting markers of oxidative and nitrosative stress and leukocyte recruitment. It was found that the single use of the NMDA antagonist kynurenic acid and its synthetic blood-brain-barrier permeable analog, SZR-72 effectively modulated the microcirculatory changes and in parallel reduced the colonic leukocyte accumulation and biochemical signs of oxido-reductive stress in the acute and subacute phases of colitis. The administration of PC also exerted potent microcirculatory effects in the intestinal mucosa; the treatment protocols normalized the altered microcirculation in the early and late phases of colitis, and a direct protective effect of dietary PC supplementation was demonstrated against injuries of the microvessel structure and vascular permeability elevations.

In conclusion, the microcirculatory inflammatory changes were successfully visualized and influenced by NMDA receptor antagonist therapy and PC administration, and the secondary, harmful consequences leading to tissue destruction were also modified. The analysis of microcirculatory reactions provided an excellent tool via which the possible anti-inflammatory, therapeutic efficacy of different, novel candidate molecules could be assessed objectively.

1. INTRODUCTION

1.1. Links between inflammation and the microcirculation

1.1.1. Characteristics of microcirculatory networks

The microcirculation includes the smallest blood vessels of an organ, the arterioles, capillaries and venules creating a microvascular network. This system has vital roles in transport, secretion and absorption; the microvessels carry O_2, nutrients, metabolic end-products, mediators and hormones to and from the tissues and cells. The microcirculatory networks additionally play decisive roles in the regulation of blood flow and pressure, and the fluid content of the tissues and the body temperature are also regulated at this level. Nevertheless, large areas of human microcirculatory biology are still unmapped, largely because of diagnostic and technical obstacles. Furthermore, the microcirculation displays many differences between species and organs, the microvascular anatomy, branching patterns, vessel densities and fine structure of capillaries may be strikingly different, and the function of the microcirculation is also highly heterogeneous.

In general, the terminal (precapillary) arterioles have an internal diameter of 15 to 20 μm and are surrounded by only one layer of smooth muscle cells. Capillaries are largely similar to a tube with an internal diameter of 4 to 10 μm, comprising a single layer of endothelial cells and a thin basement membrane. With regard to the fine structure of the endothelium, capillaries are divided into fenestrated, continuous and discontinuous categories. Capillaries drain into larger vessels that are also devoid of a smooth muscle coat. Smooth muscle appears on the media of larger venules (muscular venules) that drain the postcapillary venules.

The main cell types in the microvasculature are smooth muscle cells and adjacent endothelial cells. The endothelial lining inside the microvessels provides a smooth surface for the flow of plasma and the cellular blood components, including red blood cells and leukocytes, and regulates the movement of water and dissolved materials in the plasma between the blood and the tissues. In general, the contractile smooth muscle cells of the arterioles regulate blood flow and pressure, but the driving pressure, arteriolar tone, hemorheology and capillary patency are all important determinants of the capillary blood flow (Ince 2005).

Under normal conditions, the regulation of the microcirculation is myogenic, under metabolic or neurohormonal control (Johnson & Henrich 1975; Guslandi 1986). Myogenic control involves the sensing of strain and stress, while metabolic control involves the

regulation of O_2, CO_2, lactate and H^+ concentrations. This control uses autocrine and paracrine interactions to regulate the microcirculatory blood flow to meet the O_2 requirements of the tissue cells. The patency of the endothelium is critical in the vasomotor tone regulation by sensing the flow and metabolic regulating substances, and is actively involved in defending the body against microcirculatory dysfunctions. The arteriolar smooth muscle tone and capillary recruitment can be achieved by the release of potent vasodilator substances such as nitric oxide (NO) (Palmer *et al.* 1987) and prostacyclin, and vasoconstrictor mediators such as endothelin-1 (ET-1) (Masaki 1989) and platelet activating factor (Ince 2005).

1.1.2. Characteristics of inflammation

Inflammation is the first line of the complex protective responses to infection, irritation or cell damage by the immune system. The major distinct phases of inflammatory responses are the acute transient phase, characterized by changes in the diameter of blood vessels, local vasodilation and increased capillary permeability, followed by a slightly delayed, subacute phase, most prominently characterized by the infiltration of leukocytes and phagocytic cells, and a chronic proliferative phase, in which tissue degeneration and fibrosis occur. Many different mechanisms are involved in the inflammatory phases, but each of the classical inflammatory signs, *dolor* (pain), *calor* (heat), *rubor* (redness), *tumor* (swelling) and *functio laesa* (dysfunction of the organs involved) can be linked to changes in the microcirculation. The microcirculatory disturbance is one of the main reasons for the organ failure after the induction of inflammation, and it is considered to be based on polymorphonuclear (PMN) leukocyte-endothelial cell interactions and the increased production of reactive oxygen species (ROS) (Granger & Kubes 1994). Cytokines play a crucial role in the mediation of the inflammatory cascade signals by promoting PMN-endothelial cell interactions. In this respect the most important cytokine is tumor necrosis factor-alpha (TNF-α), which participates in a complex network of interactions in both acute and chronic inflammation (Gross *et al.* 1991; Niederau *et al.* 1997). TNF-α, produced from different types of leukocytes, is the proximal cytokine generated during an inflammatory response; it is capable of activating other cytokines and hence, remaining at the focus of the inflammation, inducing the development of a microcirculatory disturbance and excessive, systemic inflammation (Zhou *et al.* 2006; Zhou *et al.* 2008).

1.1.3. Microcirculatory consequences of inflammation

The microcirculatory network exhibits morphological and functional changes during the inflammatory response. The best characterized reactions include an impaired vasomotor

function, changes in capillary perfusion, cell to cell interactions, activation of the coagulation cascade, and increased vascular permeability (Granger 1999). These changes are based on the alterations in autoregulation of the microcirculation by inflammatory mediators.

The impaired microhemodynamics mediates further changes in inflammatory enzymes such as myeloperoxidase (MPO) and xanthine oxidoreductase (XOR), which generate ROS and cause endothelial cell damage. The functional disturbance of these enzymes, together with the activated endothelium causes an imbalance of vasoconstrictor and vasodilator molecules such as ET-1 (Masaki 1989) and NO (Palmer *et al.* 1987), evoking secondary changes in microhemodynamics and structural endothelium damage (Granger 1988). The increase in the microvascular permeability is one of the most important pathological events in the pathogenesis of inflammation. These pathophysiological events alter the barrier function and can lead to extracellular edema.

The recruitment of inflammatory cells into the perivascular tissue involves a complex cascade mechanism. The adhesion process consists of several steps, beginning with the rolling of the PMNs on the endothelial surface of the postcapillary venules until they have slowed down to such a degree that they stick to the endothelium. At this point, the PMNs are sequestered from the main vascular flow, and firm adherence to the endothelial cells may follow. Subsequently, the PMNs pass an intercellular junction between the endothelial cells and reach the abluminal side.

The most potent mediator of the intrinsic microcirculatory vasoregulation in inflammation is probably NO. This short-acting soluble gas molecule is produced from L-arginine by endothelial cells and macrophages by the enzyme nitric oxide synthase (NOS). Three major isoforms of NOS are known: endothelial NOS (eNOS or NOS1), present in vascular endothelium; neuronal NOS (nNOS or NOS3), present in the discrete neuronal populations; and a cytokine-inducible, calcium/calmodulin-independent isoform (iNOS or NOS2), expressed in various cell types when activated, including macrophages and glial cells (Moncada & Higgs 1991; Moncada *et al.* 1991). NO is a potent vasodilator and antiadhesive, and has the ability to modulate the vascular permeability (Moncada 1999; Duran *et al.* 2010). The other important component in microvascular injury is ROS formation. Oxygen-centered radicals may originate from the xanthine/xanthine oxidase system, but infiltrating PMNs also produce ROS (Granger *et al.* 1988). Further, NO can react with the superoxide anion (SOX) to form peroxynitrite, a potent oxidizing molecule capable of eliciting lipid peroxidation and cellular damage (Beckman 1990; Radi *et al.* 1991).

In general, reduced efficacy of the microcirculation results in a malfunction of the nutrient and waste product transport and leads in the long run to tissue damage. A relative lack of NO, together with the extensive release of vasoconstrictor mediators can lead to significant vasoconstriction of the precapillary sphincters, *i.e.* a considerable proportion of the inflowing blood returns to the venules without passing through the capillaries.

These alterations lead to changes in functional capillary density (FCD) and capillary red blood cell velocity (RBCV), two important parameters that can be determined by intravital microscopy (IVM). The technology allows real-time imaging of the microcirculation and the exact determination of the consequences of inflammation. FCD, an indicator of the quality of tissue perfusion, is defined as the length of red cell-perfused capillaries in relation to the observation area, which accurately describes the decrease in the efficacy of tissue perfusion when the corresponding area is unchanged (Tsai 1995). Precapillary vasoconstriction can also account for the decrease in capillary RBCV, which is determined primarily by the blood flow and the cross-section of the circulatory area. In addition to precapillary vasoconstriction, other factors, such as ROS production, can also contribute to the reduction of RBCV.

1.1.4. Microcirculatory dysfunction in gastrointestinal inflammatory disorders

Simplifying terms, such as an impaired microcirculation, are generally used to describe the microcirculatory dysfunction in pathological conditions. However, this may rather misleadingly suggest that the microcirculatory responses are uniform in nature and similar in extent. In the studies summarized in this thesis, we focused on microvascular changes in experimental models of human inflammatory disorders of the gastrointestinal (GI) tract. In this system, the mucosal layer serves as an important barrier against chemical and bacterial threats from the luminal side and modulates different bidirectional transport processes. Under normal conditions, regulation of the microcirculation is extremely complex and crucial for the transport of O_2 and nutrients in the mucous layer of the GI tract and is therefore necessary for the maintenance of normal mucosal homeostasis, intestinal permeability and the gut barrier function (Foitzik *et al.* 1999). Mucosal perfusion is mainly regulated by the vasodilators NO and prostaglandin I_2, by the sympathetic nervous system and probably by the potent vasoconstrictor ET-1. Moreover, the arterial baro- and chemoreceptors, cardiopulmonary receptors and afferents from skeletal muscle affect the GI blood flow and blood volume (Hasibeder 2010). The vascular response is a key component of GI inflammation, where tissue endothelial cells become activated, and leakiness, leukocyte

adhesiveness, procoagulant activity, and eventually angiogenesis evolve (Granger 1988; Zorov *et al.* 2006).

Inflammatory bowel diseases (IBDs) (Crohn's disease and ulcerative colitis) are chronic inflammatory conditions of the intestine and/or colon. The intracolonic application of 2,4,6-trinitrobenzenesulfonic acid (TNBS) to rodents is the most widely used experimental model of human IBD. This model is characterized by a weight loss (Morris *et al.* 1989) with visceral hyperalgesia (Zhou *et al.* 2008), significant elevations of the pro-inflammatory cytokines, including TNF-α (Neurath *et al.* 1997) and interleukin-6 (IL-6) (Ten *et al.* 2001), extensive ulcerations, morphological changes (Tatsumi & Lichtenberger 1996), significant elevations of NOS activities (Kiss *et al.* 1997; Yue *et al.* 2001) and tissue leukocyte accumulation (Kiss *et al.* 1997).

1.2. Methods for investigating the microcirculation

Investigation of the changes in the microcirculation is essential for many aspects of physiological, pathophysiological, and pharmacological studies. A number of excellent techniques are currently available for evaluation of the microcirculation. Direct investigation techniques Can be uses to measure vascular density, perfusion and blood flow; they include the side-stream dark field imaging, nailfold videomicroscopy, laser-Doppler and orthogonal polarization spectral (OPS) imaging techniques. Other, indirect investigation techniques are able topermit measurements of tissue oxygenation, *e.g.* reflectance spectroscopy, near-infrared spectroscopy, tonometry, or capnometry (De Backer *et al.* 2010). We have made use of noninvasive or minimal invasive techniques that can directly visualize or indirectly evaluate microvascular perfusion, and which are applicable under clinical conditions too.

The OPS technique is a noninvasive *in vivo* imaging method, which was developed to visualize the microcirculation directly, without the need for contrast enhancement. This technique facilitates observation of the structural pattern of the superficial microcirculation (vascular network and vessel dimensions) and quantitative measurements of physiological parameters (RBCV and perfusion of capillaries) and pathophysiological conditions, *e.g.* increased permeability. The basic feature of the OPS technique is the use of linearly polarized reflected light, which results in high-contrast images of the blood in the microcirculation. 548 nm was chosen as the wavelength of the emitted light to achieve optimal imaging, because oxy- and deoxyhemoglobin absorb light equally at this wavelength (Groner *et al.* 1999; Lindert *et al.* 2002). Incident linearly polarized light in one plane is emitted from the objective into the tissue. A second orthogonally oriented polarizer is used to block light reflected from

the tissue surfaces with unchanged polarization before visualization. Light which is multiply deflected and scattered in deeper layers of the tissue experiences a change of in polarization direction. This light passes the second polarizer and serves as a virtual light source in the depth of the tissue. Thus, images comparable to those obtained by transillumination are created (Groner *et al.* 1999; Lindert *et al.* 2002).

By means of fluorescence confocal laser scanning endomicroscopy (CLSEM), *in vivo* real-time dynamic analyses can be achieved (McLaren *et al.* 2001). The main advantage of CLSEM as compared with conventional histological investigations is that virtual biopsies can be made by an optical sectioning process, and sectioning, fixation and embedding artifacts can therefore be avoided. Three-dimensional, high-resolution optical biopsies can be obtained with this technique without the physical disruption of the observed tissue integrity on the use of systemically or topically administered fluorescent agents (Kiesslich *et al.* 2007). CLSEM involves the use of a single-line laser with a wavelength of 488 nm to generate optical histologic sections, which can be recorded at different depths within the range 0-250 μm. The optical slices are parallel with the mucosal surface with a thickness of 7 μm and a lateral resolution of 0.7 μm, the field of view being 475 μm × 475 μm. This technology is capable of providing real-time "optical" biopsy specimens in the GI tract with a very high sensitivity and specificity. It allows targeted biopsies to be taken, potentially improving the diagnostic rate in certain GI diseases. By means of this approach, the cellular and subcellular structures of the connective tissue in the colonic epithelium (surface epithelium and crypts) can examined without physical disruption of the epithelial integrity. Another advantage of this method is that the changes in the microvascular structure and damage occurring in the microvessels can be outlined as well (Kiesslich *et al.* 2007).

1.3. Therapeutic, anti-inflammatory possibilities in gastrointestinal disorders

Inflammation-induced microvascular injury can play critical roles in determining tissue survival, but the possibilities inherent in the currently used anti-inflammatory strategies are rather limited. The main emphasis at present in the therapeutics of IBDs is placed on conservative treatment. The aim of local and systemic anti-inflammatory and immunomodulant therapies is the reduction or blockage of the activation of inflammation. The medical therapy depends on the nature of the IBD, the site of the disease and the disease severity and involves anti-inflammatory aminosalicylates, corticosteroids, immunosuppressive and immunomodulatory agents (Braus & Elliott 2009) and biological therapy with monoclonal anti-TNF-α antibody (Rutgeerts *et al.* 2004). Despite advances in the

medical treatment, surgical intervention is needed in the event of ineffectiveness of conservative management or for the treatment of complications. 25-35% of patients with ulcerative colitis and 70-90% of patients with Crohn's disease will need a surgical intervention at some point during their disease (Hwang & Varma 2008).

Long-term conservative management with aminosalicylates and corticosteroids may be accompanied by severe complications, especially in the kidneys and GI tract or other severe side-effects, such as osteoporosis, hypertension, diabetes, cataract, skin striae and pathologic fractures. The main risks of immunomodulatory drugs are infections or the development of tumors. Biological therapy has much less severe and less frequent side-effects; but in the case of the administration of monoclonal anti-TNF-α antibody, up to half of the patients have no sustained benefit, due to a nonresponse, a loss of response or intolerance (Perrier & Rutgeerts 2012).

New therapeutic ways are Therefore sought, which are efficacious in improving the inflammation process, but with much milder or no side-effects.

1.3.1. The therapeutic possibilities of N-methyl-D-aspartate receptor antagonists

The main excitatory neurotransmitter in the central nervous system (CNS) is glutamate, which is also present in the enteric nervous system (ENS) (Liu *et al.* 1997; Giaroni *et al.* 2003). As concerns the several types of glutamate receptors, the N-methyl-D-aspartate (NMDA) type is expressed on a high proportion of the ENS neurons (Wiley *et al.* 1991; Sinsky & Donnerer 1998; Kirchgessner 2001; Giaroni *et al.* 2003). It has been established that the NMDA receptors play a role in the modulation of the enteric cholinergic function (Liu *et al.* 1997; Giaroni *et al.* 2003). More importantly, other *in vivo* data have shown that the expression of the NMDA receptors increases in peripheral inflammatory reactions (Tan 2008) and the receptor upregulation is present on the neurons of the myenteric plexus in TNBS-induced colitis too (Zhou *et al.* 2006).

Kynurenic acid (KynA), an antagonist of the NMDA receptors with high affinity for the glycine co-agonist site (Kessler *et al.* 1989; Stone 1993), is a product of an alternative tryptophan pathway, the major route for the conversion of tryptophan to nicotinamide adenine dinucleotide and nicotinamide adenine dinucleotide phosphate, leading to the production of a number of biologically active molecules with neuroactive properties.

L-Tryptophan is an important essential amino acid used for protein synthesis and is also a precursor of bioactive molecules. Approximately 1-2% of the intake is metabolized

through the serotonin synthesis, but most enters the kynurenine pathway, synthesizing L-kynurenine, quinolinic acid, KynA and nicotinamide adenine dinucleotide.

Two major products of the tryptophan - L-kynurenine pathway, quinolinic acid and KynA, act on glutamate receptors. Quinolinic acid is an agonist of the NMDA glutamate receptors with pro-inflammatory properties, while KynA is an endogenous NMDA receptor antagonist. KynA is able to reduce excitotoxic damage of the CNS both *in vivo* (Simon *et al.* 1986; Faden *et al.* 1989) and *in vitro* (Choi *et al.* 1988) and can be regarded as a neuroprotective agent in neurodegenerative disorders (Klivényi *et al.* 2004).

To date, a number of clinical data suggest that the metabolism of tryptophan along the kynurenine pathway is altered in inflammatory GI disorders. The plasma level of L-kynurenine is elevated in IBD patients, and the levels are likewise increased in celiac disease (Forrest *et al.* 2002; Torres *et al.* 2007). Increased serum levels of free tryptophan have been reported in patients with diarrhea-predominant irritable bowel syndrome (Christmas *et al.* 2010). These observations clearly suggest roles for NMDA-glutamate receptors and kynurenine modulation in the symptoms of inflammatory GI conditions.

An analog of KynA has recently been synthetized SZR-72, which differs from KynA mainly in that it can cross the blood-brain barrier. It was originally developed to influence NMDA receptor overexcitation in the CNS, but its role and peripheral effects on the ENS are still largely unmapped (Fülöp *et al.* 2009).

1.3.2. The therapeutic possibilities of phosphatidylcholine

Phosphatidylcholine (PC), a ubiquitous phospholipid, is a major component of biomembranes, and a number of experimental and clinical studies have demonstrated that it alleviates the consequences of inflammation and ischemia in different organs and experimental models (Stremmel *et al.* 2005; Erős *et al.* 2006; Gera *et al.* 2007; Ghyczy *et al.* 2008; Tőkés *et al.* 2011). Furthermore, it inhibits the mucosal damage and morphologic impairment caused by acids and other noxious agents in the GI tract (el-Hariri *et al.* 1992; Erős *et al.* 2006). Compelling *in vitro* evidence has been published that exogenous PC significantly inhibits TNF-α-induced inflammatory responses (Treede *et al.* 2007).

In vivo, PC is produced via two major pathways. Two fatty acids undergo addition to glycerol phosphate, to generate phosphatidic acid. This is converted to diacylglycerol, after which phosphocholine (the head group) is added to give cytidine 5-diphosphocholine. The second, minor pathway involves the methylation of phospatidylethanolamine, in which three methyl groups are added to the ethanolamine head-group of the phospholipids, converting it

into PC. Orally taken PC serves as a slow-release blood choline source. The choline component of PC participates in a wide range of responses, including interference with the mechanism of activation of the PMNs (Monje *et al.* 2003) and this pathway becomes important under inflammatory stress conditions. Choline itself is anti-inflammatory; PC is taken up by phagocytic cells, and it may accumulate in inflamed tissues (Cleland *et al.* 1979). On the other hand, the hydrolysis of PC by phospholipase D generates choline in cholinergic neurons (Blusztajn & Wurtman 1983), and this choline is used for synthesis of the principal vagal neurotransmitter, acetylcholine. Previous studies have shown that some of the choline is stored in the form of membrane PC, and this pathway may become particularly important when extracellular circulating choline concentrations are low (*e.g.* during a dietary choline deficiency) or when acetylcholine synthesis and release are accelerated by high neuronal activity (Ulus *et al.* 1989; Lee *et al.* 1993).

2. MAIN GOALS

Examination of the local microcirculatory function or a dysfunction within affected tissues is critical to determine the efficacy of therapeutic approaches in inflammatory pathologies. Agents which improve the function of the microcirculation might be more promising therapeutics and more advantageous in clinical practice. In our investigations, we specifically focused on new, possible therapeutic ways which could be efficacious in mitigation of the inflammation process through their microvascular and microcirculatory effects. The main goals were to evaluate the degree of inflammatory activation together with the GI microcirculatory changes in experimental models of colitis, and to test new methods via which to influence such events simultaneously. In this line, our aims were:

1. to evaluate the usefulness of microcirculatory imaging for recognition of the microcirculatory dysfunction and microvessel injuries caused by inflammation in the GI tract in experimental models of IBD;
2. to compare the potential applications of OPS and CLSEM techniques in the GI tract;
3. to develop a new scoring system with which to estimate the rate of microcirculatory changes under experimental conditions;
4. to study the microcirculatory effects and anti-inflammatory properties of NMDA-antagonist treatment modalities in experimental colitis;
5. to examine the anti-inflammatory effects of oral PC treatment regimens on the colitis-induced microcirculatory changes and tissue damage in this condition.

3. MATERIALS AND METHODS

The experimental protocol was approved by the Ethical Committee for the Protection of Animals in Scientific Research at the University of Szeged and followed the NIH guidelines for the care and use of experimental animals.

3.1. Animals

The animals, fed on a normal diet with tap water available *ad libitum,* were divided into two studies. The experiments in Study I were performed on 32 (280-320 g) male Wistar rats (Series 1), and 32 (280-320 g) male Sprague-Dawley rats (Series 2). In Study II, 48 male Sprague-Dawley rats were used. The animals were housed in plastic cages in a thermoneutral environment (21 ± 2 °C) with a 12-h dark-light cycle.

3.2. Induction of colitis

The animals were deprived of food, but not water, for 12 h prior to the enema. Colonic inflammation was induced by the intracolonic administration of TNBS (40 mg kg^{-1} in 0.25 ml of 25% ethanol) through an 8-cm-long soft plastic catheter under transient ether anesthesia (Morris *et al.* 1989). In sham-operated groups, only the vehicle for TNBS was administered. The animals were then returned to their cages and were fed *ad libitum* with standard laboratory chow.

3.3. Surgical preparation

The animals were anesthetized with sodium pentobarbital (50 mg kg^{-1} bw *ip*) 1 or 6 days after the enema and placed in a supine position on a heating pad. Tracheostomy was performed to facilitate spontaneous breathing, and the right jugular vein was cannulated with PE50 tubing for fluid administration and Ringer's lactate infusion (10 ml kg^{-1} h^{-1}) during the experiments. A thermistor-tip catheter (PTH-01; Experimetria Ltd., Budapest, Hungary) was positioned into the ascending aorta through the right common carotid artery to measure the cardiac output (CO) by a thermodilution technique. The right femoral artery was cannulated with PE40 tubing for mean arterial pressure (MAP) and heart rate (HR) measurements.

3.4. Direct measurements of the microcirculation

3.4.1. Intravital videomicroscopy

The OPS imaging technique (Cytoscan A/R, Cytometrics, Philadelphia, PA, USA) was used for noninvasive visualization of the serosal microcirculation of the colon. This technique utilizes reflected polarized light at the wavelength of the isobestic point of oxy- and deoxyhemoglobin (548 nm). As polarization is preserved in reflection, only photons scattered

from a depth of 2-300 μm contribute to image formation. A 10x objective was placed onto the serosal surface of the ascending colon, and microscopic images were recorded with an S-VHS video recorder 1 (Panasonic AG-TL 700; Matsushita Electric Ind. Co. Ltd, Osaka, Japan). Quantitative assessment of the microcirculatory parameters was performed off-line by frame-to-frame analysis of the videotaped images. RBCV (μm s^{-1}) changes in the postcapillary venules were determined in three separate fields by means of a computer-assisted image analysis system (IVM Pictron, Budapest, Hungary).

3.4.2. In vivo detection of microvascular damage

The extent of microvascular damage of the distal colon was evaluated with CLSEM (Five1; Optiscan Pty. Ltd., Melbourne, Victoria, Australia) developed for *in vivo* histology. This technique is capable of determining the vascular permeability. The analysis was performed twice, separately by two investigators. The mucosal surface of the distal colon 8 cm proximal to the anus was surgically exposed and laid flat for examination. The microvascular structure was recorded after the *iv* administration of 0.3 ml of fluorescein isothiocyanate-dextran (FITC-dextran 150 kDa, 20 mg ml^{-1} solution dissolved in saline, Sigma). The objective of the device was placed onto the mucosal surface of the descending colon, and confocal imaging was performed 5 min after dye administration (1 scan/image, 1024 x 512 pixels and 475 x 475 μm per image). The degree of edema was examined following topical application of the fluorescent dye acridine orange (Sigma-Aldrich Inc, St. Louis, MO, USA) in the mucosal architecture. The surplus dye was washed off the mucosal surface of the colon with saline 2 min before imaging. The CLSEM imaging technique was used in, Study I and Study II.

Non-overlapping fields of active areas of disease were processed in TNBS-treated animals and compared with the control group by using a semiquantitative scoring system. The grading was performed with two criteria: 1. the structure of the microvessels (0 = normal, 1 = dye extravasation, but the vessel structure was recognizable, 2 = destruction, and the vessel structure was unrecognizable), 2. edema (0 = no edema, 1 = moderate epithelial swelling, 2 = severe edema).

3.5. Detection of inflammatory markers

3.5.1. Preparation of tissue biopsies

Tissue biopsies kept on ice were homogenized in phosphate buffer (pH 7.4) containing Tris-HCl (50 mM, Reanal, Budapest, Hungary), EDTA (0.1 mM), dithiotreitol (0.5 mM), phenylmethylsulfonyl fluoride (1 mM), soybean trypsin inhibitor (10 μg ml^{-1}) and leupeptin

(10 µg ml^{-1}, Sigma-Aldrich GmbH, Steinheim, Germany). The homogenate was centrifuged at 4 °C for 20 min at 24 000 g (Amicon Centricon-100, Millipore Corporation, Bedford, MA, USA). Tissue nitrite, nitrate and nitrotyrosine and XOR activity were determined in the supernatant, while MPO activity was measured in the pellet of the homogenate.

3.5.2. Tissue MPO activity

The activity of MPO as a marker of tissue leukocyte infiltration was measured on the pellet of the homogenate by the modified method of Kuebler *et al,* (Kuebler *et al.* 1996). Briefly, the pellet was resuspended in K$_3$PO$_4$ buffer (0.05 M; pH 6.0) containing 0.5% hexa-1,6-bis-decyltriethylammonium bromide. After three repeated freeze-thaw procedures, the material was centrifuged at 4 °C for 20 min at 24,000 g and the supernatant was used for MPO determination. Subsequently, 0.15 ml of 3,3',5,5'-tetramethylbenzidine (dissolved in DMSO; 1.6 mM) and 0.75 ml of hydrogen peroxide (dissolved in K$_3$PO$_4$ buffer; 0.6 mM) were added to 0.1 ml of the sample. The reaction led to the hydrogen peroxide-dependent oxidation of tetramethylbenzidine, which could be detected spectrophotometrically at 450 nm (UV-1601 spectrophotometer; Shimadzu, Kyoto, Japan). MPO activities were measured at 37 °C; the reaction was stopped after 5 min by the addition of 0.2 ml of H$_2$SO$_4$ (2 M) and the resulting data were referred to the protein content.

3.5.3. Tissue XOR activity

The XOR activity was determined in the ultrafiltered, concentrated supernatant by a fluorometric kinetic assay based on the conversion of pterine to isoxanthopterine in the presence (total XOR) and absence (xanthine oxidase activity) of the electron acceptor methylene blue (Beckman *et al.* 1989).

3.5.4. Measurement of tissue NO products

Nitrite and nitrate (NO$_x$), stable end-products of NO, were determined in the colonic homogenate by the Griess reaction. This assay depends on the enzymatic reduction of nitrate to nitrite, which is then converted into a colored azo compound detected spectrophotometrically at 540 nm. Total NO$_x$ was calculated and expressed as µmol (mg protein)$^{-1}$ (Moshage *et al.* 1995).

3.5.5. NOS activity

NO formation in the colonic tissue was measured by the conversion of [^{3}H]L-citrulline from [^{3}H]L-arginine according to a published method (Szabó *et al.* 1993). Briefly, tissue biopsies kept on ice were homogenized in phosphate buffer (pH = 7.4) containing 50 mM tris(hydroxymethyl)aminomethane-HCl (Reanal, Budapest, Hungary), 0.1 mM

ethylenediaminetetraacetic acid (Serva Feinbiochemica GmbH, Heidelberg, Germany), 0.5 mM dithiotreitol, 1 mM phenylmethylsulfonyl fluoride and 10 μg ml^{-1} soybean trypsin inhibitor. The homogenate was centrifuged at 4 °C for 20 min at 24,000 g and the supernatant was loaded into centrifugal concentrator tubes (Amicon Centricon-100; 100,000 MW cutoff ultrafilter). The tubes were centrifuged at 1,000 g for 150 min and the concentrated supernatant was washed out from the ultrafilter with 300 μl of homogenizing buffer. The samples were incubated with cation-exchange resin (Dowex AG 500W-X8, Na$^+$ form) for 5 min to deplete endogenous L-arginine. The resin was separated by centrifugation (1,500 g for 10 min) and the supernatant containing the enzyme was assayed for NOS activity.

For the Ca^{2+}-dependent NOS activity, 50 μl of enzyme extract and 100 μl of reaction mixture (pH 7.4, containing 50 mM Tris-HCl buffer, 1 mM NADPH, 10 μM tetrahydrobiopterin, 1.5 mM CaCl$_2$, 100 U ml^{-1} calmodulin and 0.5 μCi [^{3}H]L-arginine (ICN Biomedicals; specific activity 39 Ci mmol^{-1}) were incubated together for 30 min at 37 °C. The reaction was stopped by the addition of 1 ml of ice-cold HEPES buffer (pH 5.5) containing 2 mM EGTA and 2 mM EDTA. Measurements were performed with boiled enzyme and with the NOS inhibitor N-ω-nitro-L-arginine (3.2 mM) to determine the extent of [^{3}H]L-citrulline formation independent of the NOS activity. Ca^{2+}-independent NOS activity (iNOS) was measured without Ca-calmodulin and with EGTA (8 mM).

1 ml of reaction mixture was applied to Dowex cation-exchange resin (AG 50WX8, Na$^+$ form) and eluted with 2 ml of distilled water. The eluted [^{3}H]L-citrulline activity was measured with a scintillation counter (Tri-Carb Liquid Scintillation Analyzer 2100TR/2300TR; Packard Instrument Co., Meriden, CT., USA).

3.5.6. Immunoassay for tissue nitrotyrosine

Free nitrotyrosine, as a marker of peroxynitrite generation, was measured by enzyme-linked immunosorbent assay (ELISA; Cayman Chemical; Ann Arbor, MT, USA). Large intestinal tissue samples were homogenized and centrifuged at 15,000 g. Supernatants were collected and incubated overnight with anti-nitrotyrosine rabbit IgG and nitrotyrosine acetylcholinesterase tracer in precoated (mouse anti-rabbit IgG) microplates, followed by development with Ellman's reagent. Nitrotyrosine content was normalized to the protein content of the small intestinal homogenate and expressed in ng (mg protein)$^{-1}$.
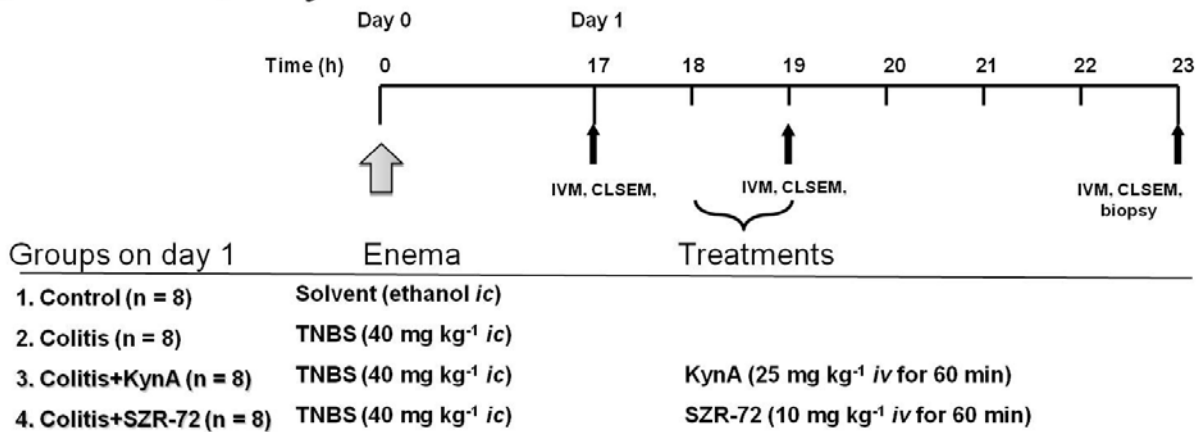
3.6. Experimental protocol, Study I

In Series 1, 32 animals were randomly allocated into 4 groups. The animals received enemas with a total volume of 0.25 ml containing only the solvent (25% ethanol) in the case

of group 1 (n = 8), which was the control group. In groups 2-, 3- and 4 (n = 8, each) colitis was induced with an enema of TNBS (40 mg kg^{-1} in solvent). On the following day, the animals were anesthetized and surgery was performed to monitor the hemodynamic parameters for 6 h, starting 17 h after the enemas. Group 2 served as untreated colitis group, while in group 3 the animals were treated *iv* with 25 mg kg^{-1} KynA (Sigma Chem, St Louis, MO, USA) dissolved in 0.1 M NaOH with the pH adjusted to 7.2-7.4. Group 4 received *iv* 10 mg kg^{-1} of SZR-72 in a 1 ml h^{-1} infusion for 60 min. SZR-72 (2-(2-N,N-dimethylaminoethylamine-1-carbonyl)-1H-quinolin-4-one hydrochloride, synthetized by the Institute of Pharmaceutical Chemistry, University of Szeged (Patent No. 104448-1998/Ky/me), was dissolved in 1 ml of saline and the pH was adjusted to 7.2-7.4. The infusion of KynA or SZR-72 started 60 min after the end of surgery, 18 h after the intracolonal instillation of TNBS or the solvent, and lasted for 60 min (summarized in Figure 1).

In the second part of Study I (Series 2), the animals were also allotted to 4 groups (n = 8 in each group). The experimental set-up was identical on day 6 in the subacute phase of TNBS colitis in this series. Group 5 was the control group, while in groups 6-, 7- and 8 colitis was induced. The hemodynamic measurements were started 6 days following the TNBS enema. The animals in groups 7 and 8 received KynA or SZR-72, respectively.

In Series 1, the animals in groups 1-4 were anesthetized 1 day after the TNBS enema; in Series 2, the animals of groups 5-8 were anesthetized 6 days after colitis induction. Surgery was performed to allow registration of the hemodynamic parameters at 1-h intervals for 6 h (CO data were measured only at the end of the experiments). IVM was performed at the end of the experiments to visualize the serosal microcirculation 3 cm distal from the cecum. Additionally, CLSEM was performed to examine the changes in microvasculature of the mucosa of the distal colon. At the end of the experiments, full-thickness tissue samples were taken to determine the colonic MPO and NOS activities in Series 1, and the tissue MPO activity and plasma NO$_x$ level in Series 2 (the protocol is summarized in Figure 1).
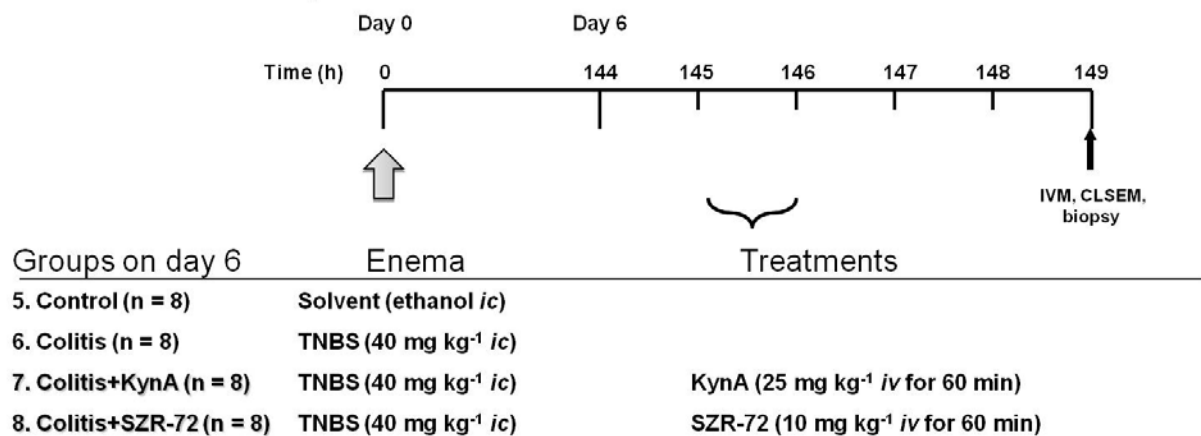
Figure 1. Experimental protocol of Study I. Time sequence of treatments and measurements in Series 1 and 2.

3.7. Experimental protocol, Study II

In the first part of the studies, 24 animals were randomly allocated into 3 groups. Group 1 (n = 8) served as sham-operated controls; the animals received enemas with the solvent for TNBS (25% ethanol in a total volume of 0.25 ml) and were nourished with standard laboratory chow. The group 2 animals (n = 8) were kept on a standard laboratory diet for 6 days and colitis was then induced with a TNBS enema. In group 3 (n = 8), the animals were fed with a special diet (Ssniff Spezialdiäten; Germany) containing 2% PC (1,2-diacylglycero-3-phosphocholine; R45; Lipoid GmbH, Ludwigshafen, Germany) for 6 days prior to the TNBS enema. In these groups, the experiments were started with baseline hemodynamic measurements 1 day after TNBS induction (summarized in Figure 2).

The experimental set-up was identical on day 6 in the subacute phase of TNBS colitis.

Group 4 (n = 8) nourished with standard laboratory chow, served as the sham-operated group; the enema was performed with the solvent of TNBS. In group 5 (n = 8), colitis was induced with the TNBS enema 6 days before the measurements, and these animals were fed with standard laboratory chow. In group 6 (n = 8), colitis was induced with the TNBS enema 6 days before the start of the observations, and the animals were fed with the 2% PC-enriched diet for 3 days before and 3 days after the TNBS enema. The hemodynamic measurements were started 6 days following the TNBS enema (summarized in Figure 2).

In Series 1, the animals in groups 1-3 were anesthetized 1 day after the TNBS enema; in Series 2, groups 4-6 were anesthetized 6 days after colitis induction. Surgery was performed to allow registration of the hemodynamic parameters at 1-h intervals for 6 h (CO data were measured only at the end of the experiments). IVM was performed at the end of the experiments to visualize the serosal microcirculation 3 cm distal from the cecum. Additionally, CLSEM was performed to examine the changes in microvasculature of the mucosa of the distal colon, and full-thickness tissue samples and venous blood samples were taken to determine the biochemical changes (tissue MPO and XOR activity) in the colon and plasma.

Series 1 of Study II

Groups	Diet	Enema	Examinations
1. Control (n = 8)	Normal chow	Solvent (ethanol *ic*)	Hemodynamics, IVM, CLSEM, biopsy
2. Colitis (n = 8)	Normal chow	TNBS (40 mg kg^{-1} *ic*)	
3. Colitis+PC (n = 8)	PC-enriched diet	TNBS (40 mg kg^{-1} *ic*)	

Day - 6   Day 0   Day 1

Series 2 of Study II

Groups	Diet	Enema	Examinations
4. Control (n = 8)	Normal chow	Solvent (ethanol *ic*)	
5. Colitis (n = 8)	Normal chow	TNBS (40 mg kg^{-1} *ic*)	
6. Colitis+PC (n = 8)	PC-enriched diet	TNBS (40 mg kg^{-1} *ic*)	

Day - 3   Day 0   Day 3   Day 6

Figure 2. Experimental protocol of Study II. Time sequence of treatments and measurements in Series 1 and 2 of Study II.

3.8. Statistical analysis
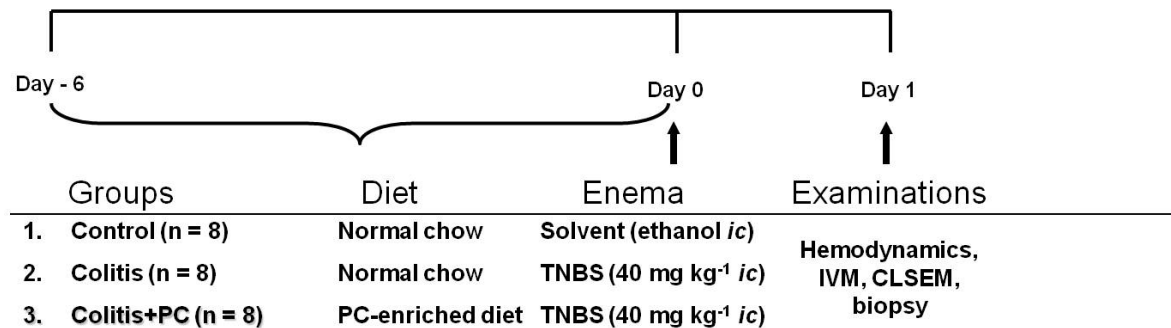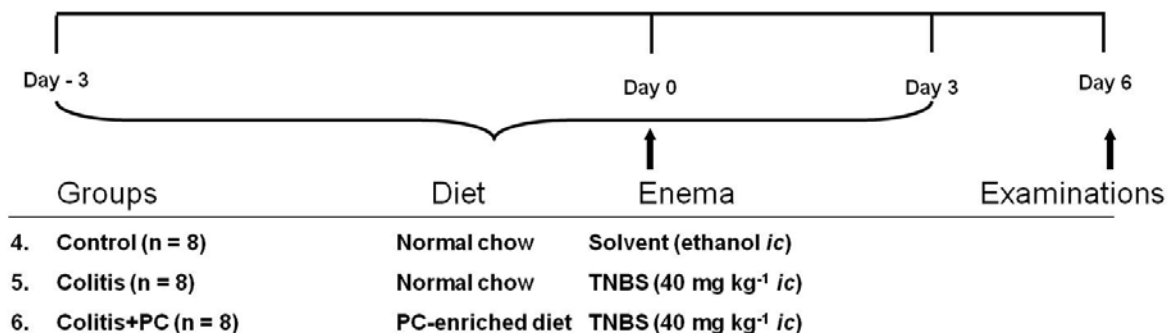
In all studies, data analysis was performed with a statistical software package (SigmaStat for Windows; Jandel Scientific, Erkrath, Germany). The distribution of our experimental data was analyzed by the Kolmogorov-Smirnov normality test. Failure of the normality test indicated nonparametric distribution of the data. Accordingly, we employed nonparametric statistical tests. Friedman repeated measures analysis of variance on ranks was applied within groups. Time-dependent differences from the baseline for each group were assessed by Dunn's method. Differences between groups were analyzed with Kruskal-Wallis one-way analysis of variance on ranks, followed by Dunn's method for pairwise multiple comparison. In the Figures, median values and 75th and 25th percentiles are given; p values < 0.05 were considered significant.

4. RESULTS

4.1. Study I

4.1.1. Hemodynamics

In Series 1, there were no significant changes in the hemodynamic parameters as compared with the baseline values in the sham-operated group during the observation period. The CO was significantly higher in the colitis groups than in the sham-operated group, while the MAP and TPR (total peripheral resistance) were significantly lower in the TNBS-treated groups than in the control group (Annex 1, Figures 1-2 and Table 1).

Treatment with KynA did not influence the colitis-induced changes in MAP, CO and TPR as compared with the colitis group (Annex 1, Figures 1 and 2 and Table 1). After SZR-72 treatment, a significant increase in TPR relative to the colitis group evolved subsequent to 19 h after colitis induction (Annex 1, Figures 1 and 2 and Table 1). The carotid artery flow was measured to estimate the condition of the cerebral perfusion. Neither TNBS-induced colitis, nor KynA or SZR-72 treatment influenced the carotid artery flow or HR (Annex 1, Table 1).

In Series 2, the carotid artery flow was significantly higher in the colitis group than in the sham-operated group, but there were no significant changes in between-group differences in MAP, CO or TPR under the baseline conditions 6 days after the vehicle enema instillation or colitis induction, before the start of NMDA receptor antagonist treatment. The increased carotid flow was significantly decreased by SZR-72 treatment, but the other macrohemodynamic parameters were not influenced by the administration of the NMDA receptor inhibitors (Annex 4, Table 1).

4.1.2. The microcirculation

The RBCV of the serosa was examined as a quantitative marker of the colonic microcirculatory condition. In Series 1, the RBCV was significantly increased in the colitis group as compared with the control group. KynA and SZR-72 both significantly decreased the colitis-induced elevation in RBCV on day 1. However, the SZR-72 treatment was the more effective in decreasing the inflammation-caused RBCV elevation (Figure 4A).

Six days after the TNBS enema, the RBCV in the colonic subserosa was significantly increased in the colitis group as compared with the sham-operated control group. KynA administration did not influence this change significantly, while SZR-72 treatment decreased the elevated RBCV by the end of the observation period (Figure 4B).
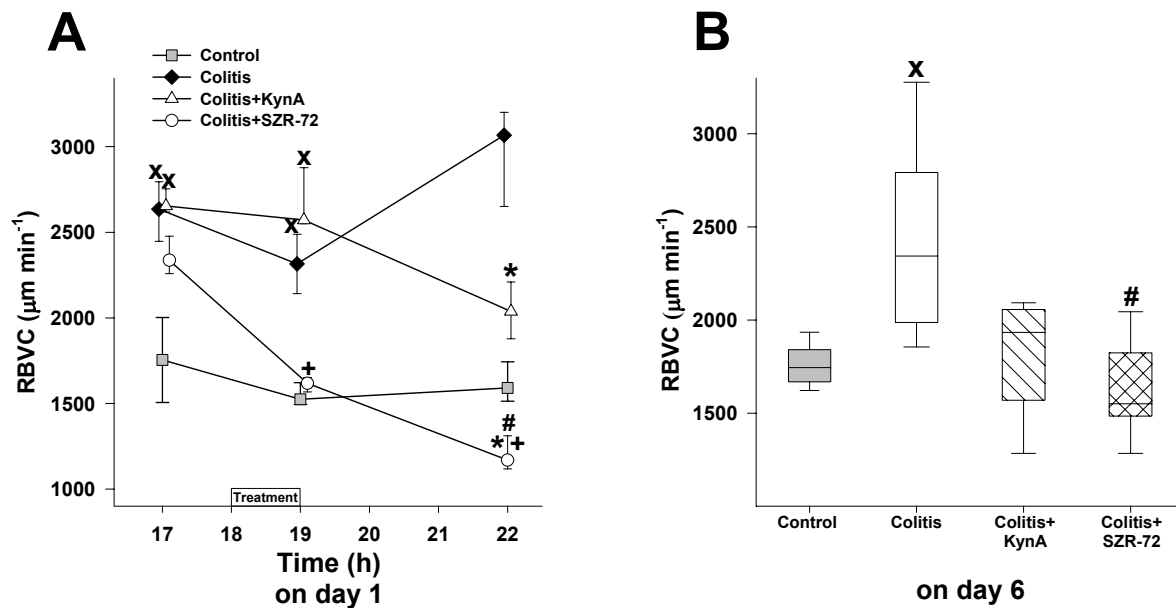
Figure 4. A: *Changes in RBCV in the control (shaded squares with a thin continuous line), colitis (black diamonds with a thick line), SZR-72 (empty circles with a thick line) and KynA-treated colitis (empty triangles with a thick line) groups. The box indicates the treatment with NMDA antagonists. The plots demonstrate the median values and the 25th (lower whisker) and 75th (upper whisker) percentiles; * $p < 0.05$ within groups vs baseline values, ^{x} $p < 0.05$ between groups vs control group values, $^{#}$ $p < 0.05$ between NMDA antagonist-treated groups vs colitis group, $^{+}$ $p < 0.05$ KynA-treated group vs SZR-72-treated group values.* **B:** *Changes in RBVC in the sham-operated control (shaded box), colitis (empty box), KynA-treated colitis (striped box) and SZR-72-treated (checked box) groups on day 6 of colitis. The plots demonstrate the median (horizontal line in the box) and the 25th and 75th percentiles. ^{x} $p < 0.05$ between colitis group and control group values, $^{#}$ $p < 0.05$ between colitis+NMDA antagonist-treated group and colitis group values.*

4.1.3. Biochemical data

4.1.3.1. MPO activity

The TNBS enema caused tissue leukocyte accumulation both on day 1 and on day 6 of colitis, as determined via measurement of the MPO activity.

The median MPO activity in the control animals at the end of the observation period in Series 1 was 740 mU (mg protein)$^{-1}$. 23 h after colitis induction, the MPO activity was increased significantly in the proximal colon relative to the control group. Each of the NMDA antagonist treatments resulted in a significant decrease in the MPO activity of the large bowel

as compared with the nontreated colitis group (Figure 5A).

In Series 1, the MPO activity was significantly elevated 6 days after colitis induction (M = 854; p25 = 696; p75 = 1156 mU (mg protein)$^{-1}$ *vs* the control M = 438; p25 = 363; p75 = 576 mU (mg protein)$^{-1}$). KynA administration decreased the MPO activity significantly in the large bowel in comparison with the nontreated colitis group (M = 523; p25 = 373; p75 = 638 mU (mg protein)$^{-1}$). The SZR-72 treatment also decreased the MPO activity, but less effectively (M = 752; p25 = 654; p75 = 824 mU (mg protein)$^{-1}$) (Figure 5B).
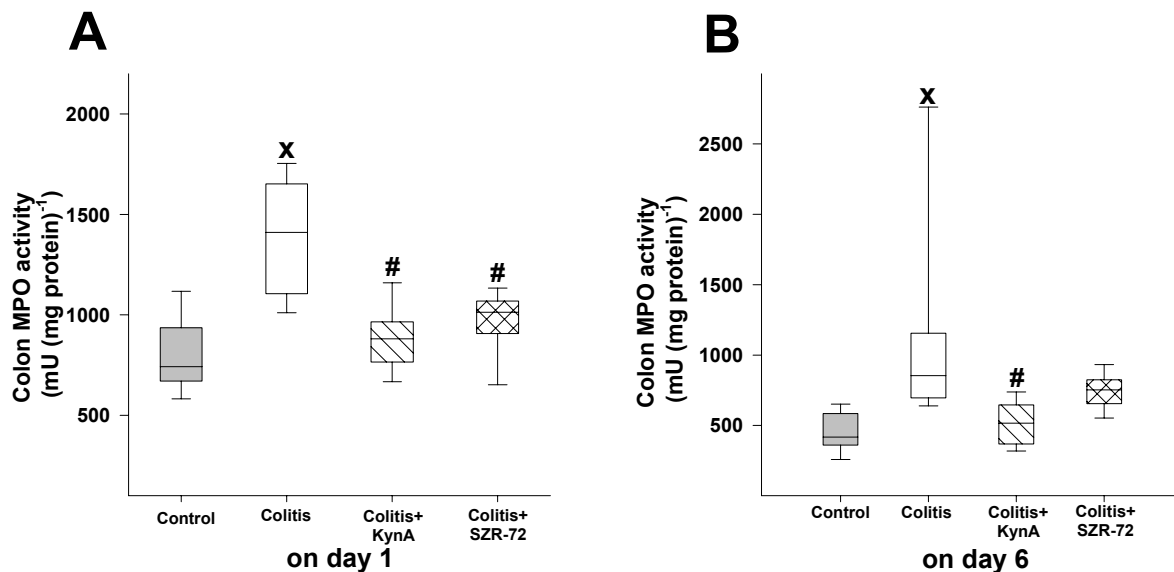

Figure 5. *Changes in activity of MPO in Series 1 (**A**) and Series 2 (**B**) in colonic tissue from the control (shaded box), colitis (empty box), KynA-treated colitis (striped box) and SZR-72-treated (checked box) groups. The plots demonstrate the median (horizontal line in the box) and the 25th (lower whisker), and 75th (upper whisker) percentiles. ^{x} p < 0.05 between groups and control group values, $^{#}$ p < 0.05 between NMDA antagonist-treated groups and colitis group values.*

4.1.3.2. NOS activity, tissue NO$_x$ levels and tissue nitrotyrosine levels

NOS activity is responsible for the production of NO, an important regulator of the colonic microcirculation. On day 1 of colitis, the TNBS enema resulted in a significant increase in the total NOS activity over the value for the control group. Both of the NMDA antagonist treatments significantly decreased the colonic NOS activity as compared with the nontreated colitis group (Figure 6A).

In Series 2, NO$_x$ and nitrotyrosine levels were measured. On day 6 of colitis, a significant elevation was observed in the NO$_x$ level in the colonic tissue of the colitis group relative to the control group. Both NMDA antagonists decreased the NO$_x$ levels to the control

level (Figure 6B).

The interaction of NO with SOX produces peroxynitrite, which causes the nitration of proteins and amino acid residues such as tyrosine. Whereas NO has a short half-life, the nitrotyrosine epitopes are stable and tend to accumulate in inflammatory surroundings. The nitrotyrosine levels were significantly elevated in the colitis group as compared with the sham-operated group, and both NMDA antagonists effectively decreased the amount of nitrotyrosine in the colonic tissue (Figure 6C).
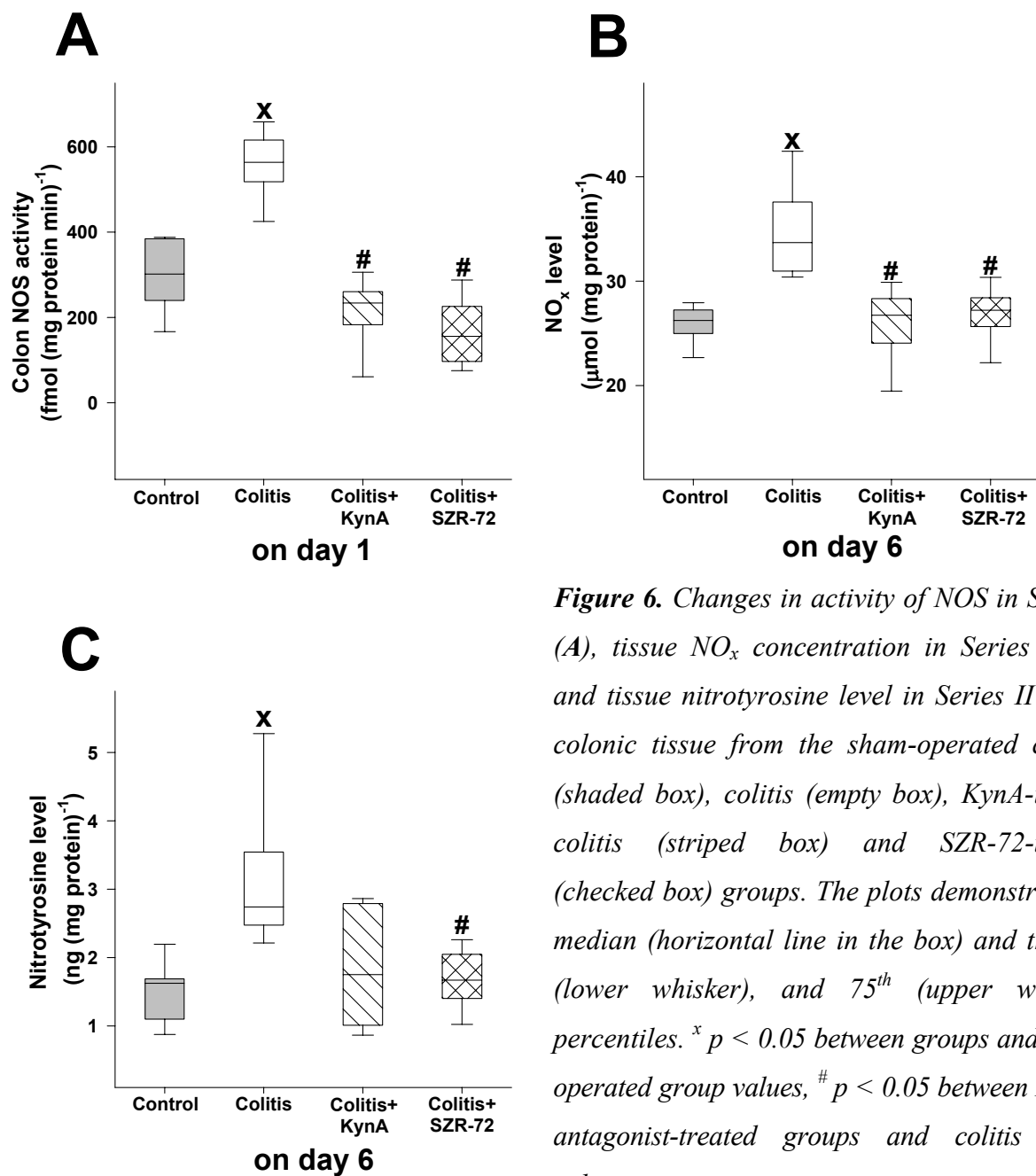
Figure 6. Changes in activity of NOS in Series I (A), tissue NO_x concentration in Series II (B) and tissue nitrotyrosine level in Series II (C) in colonic tissue from the sham-operated control (shaded box), colitis (empty box), KynA-treated colitis (striped box) and SZR-72-treated (checked box) groups. The plots demonstrate the median (horizontal line in the box) and the 25th (lower whisker), and 75th (upper whisker) percentiles. $^x p < 0.05$ between groups and sham-operated group values, $^{\#} p < 0.05$ between NMDA antagonist-treated groups and colitis group values.

4.1.3.3. In vivo detection of microvessel damage

The colonic microvessels were visualized by FITC-dextran administration and edema formation was determined by topical application of acridine orange dye. In the control groups on day 1 and day 6 of colitis the network of capillaries exhibited a typical honeycomb pattern (M = 0; p25 = 0; p75 = 0.275; Figures 7A and 7E). In both Series, significant vessel damage was detected by CLSEM. One day after colitis induction, the capillary network was disorganized, the honeycomb pattern had disappeared, and fluorescent dye leakage was observed in several areas of the large intestine. A damaged capillary endothelium with edema formation was generally observed (M = 4; p25 = 3.25; p75 = 4; Figure 7B). In series 2, TNBS enema caused disorganized capillary network and fluorescent dye leakage in the colon (M = 2; p25 = 1.625; p75 = 2.375; Figure 7F). After treatment with KynA (Figure 7C on day 1; Figure 7G on day 6) or SZR-72 (Figure 7D on day 1; Figure 7H on day 6), the level of injury did not differ markedly between the groups and the NMDA antagonist treatment did not influence the structural changes in the microvasculature of the inflamed colonic mucosa significantly in either Series 1 or Series 2.
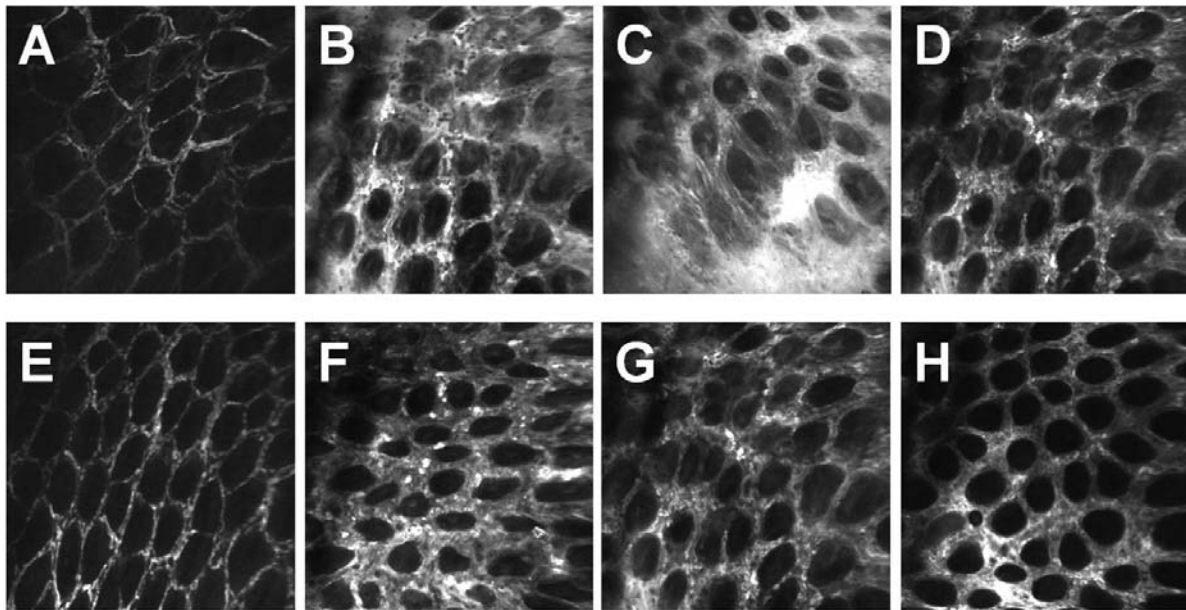
Figure 7. *In vivo histology images of the mucosal surface of the distal rat colon, recorded by CLSEM after iv administration of FITC-dextran. **A:** Normal mucosal vasculature of the distal colon. **B:** One day after the TNBS enema instillation, dye leakage is observed from the vessel lumina, and the normal honeycomb pattern of the capillaries has disappeared in the colitis group. **C**: One day after TNBS enema instillation in the KynA-treated colitis group, dye leakage is observed from the vessel lumina, and the normal honeycomb pattern of the capillaries has disappeared. **D:** One day after TNBS enema instillation in the SZR-72-treated*

*colitis group, dye leakage is observed from the vessel lumina, and the normal honeycomb pattern of the capillaries has disappeared. **E:** Normal mucosal vasculature of the distal colon 6 days after instillation of the TNBS solvent **F:** Six days after the TNBS enema instillation, dye leakage is observed from the vessel lumina, and the normal honeycomb pattern of the capillaries has disappeared in the colitis group. **G**: Six days after TNBS enema instillation in the KynA-treated colitis group, dye leakage is observed from the vessel lumina, and the normal honeycomb pattern of the capillaries has disappeared. **H:** Six days after TNBS enema instillation in the SZR-72-treated colitis group, dye leakage is observed from the vessel lumina, and the normal honeycomb pattern of the capillaries has disappeared.*

4.2. Study II

4.2.1. Hemodynamics

There were no significant changes in the hemodynamic parameters as compared with the baseline values in the sham-operated groups during the observation periods. In Series 1, the MAP values were significantly lower in the colitis group than in the sham-operated group. PC feeding normalized this elevation (Annex 3, Figure 2A). CO was significantly higher as compared with the sham-operated group and the PC feeding did not influence the colitis-induced changes in CO as compared with the colitis group (Annex 3, Figure 2B). There were no significant changes in the HR values in any of the three groups (data not shown).

In series 2, there were no significant differences between the groups in the MAP, CO or HR changes 6 days after the vehicle enema or colitis induction (Annex 3, Figures 2A, B).

4.2.2. The microcirculation

The RBCV in the subserosa of the colon was significantly increased on days 1 and 6 of colitis as compared with the control groups. PC administration normalized the colitis-induced elevation in RBCV in Series 1, but did not cause a significant reduction of RBCV, in contrast with the colitis group in Series 2 (Figure 8).
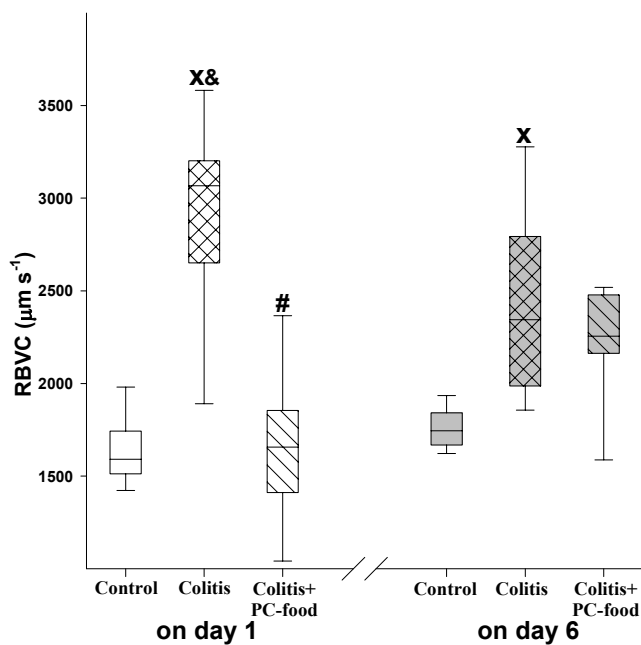
Figure 8. Changes in RBCV in colonic serosa on day 1 in the control (white box), colitis (checked white box) and PC-pretreated colitis (striped white box) groups; and on day 6 in the control (empty gray box), colitis (checked gray box) and PC-pretreated colitis (striped gray box) groups. The plots demonstrate the median (horizontal line in the box) and the 25th (lower whisker) and 75th (upper whisker) percentiles. ^{x} p < 0.05 between groups and control group on day 1, $^{\&}$ p < 0.05 between groups and control group on day 6, $^{\#}$ p < .05 between PC-pretreated group and colitis group on day 1.

4.2.3. Biochemical data

4.2.3.1. XOR activity

The mucosal XOR is activated during inflammation processes and produces a considerable amount of SOX radical. The XOR activity was significantly higher 1 and 6 days after colitis induction as compared with the control groups. In both cases, the PC-enriched diet effectively decreased the XOR activity in the large bowel in comparison with the nontreated controls (Figure 9A).

4.2.3.2. MPO activity

The TNBS enema caused tissue leukocyte accumulation in the proximal colon on days 1 and 6, as determined via the MPO activity. In both cases, PC feeding decreased the MPO activity significantly in the large bowel. In Series 2, the MPO activity of the PC-treated group was decreased significantly, in contrast with the colitis group on day 6 and also with the PC-pretreated group on day 1 (Figure 9B).
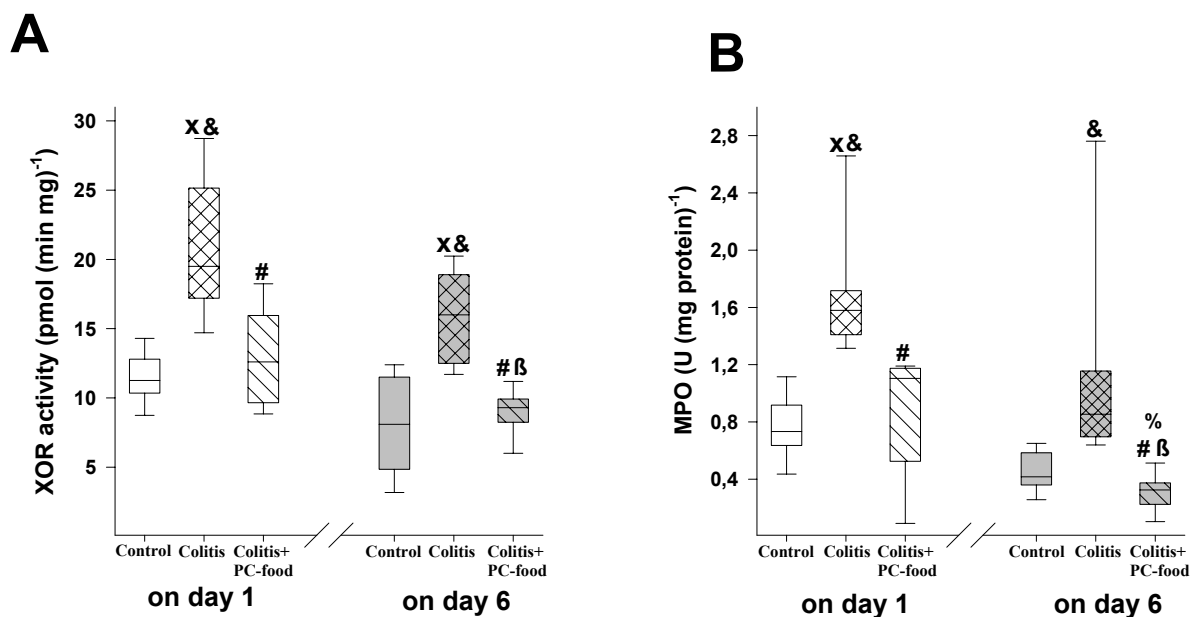
Figure 9. *Changes in XOR activity (A) and MPO activity (B) on day 1 in the control (white box), colitis (checked white box) and PC-pretreated colitis (striped white box) groups; and on day 6 in the control (empty gray box), colitis (checked gray box) and PC-pretreated colitis (striped gray box) groups. The plots demonstrate the median (horizontal line in the box) and the 25th (lower whisker) and 75th (upper whisker) percentiles. ^{x} p < 0.05 between groups and control group on day 1, $^\&$ p < 0.05 between groups and control group on day 6, $^\#$ p < 0.05 between PC-pretreated groups and colitis group on day 1, $^\beta$ p < 0.05 between PC-pretreated groups and colitis group on day 6, $^\%$ p < 0.05 between PC-pretreated group on day 1 and PC-*

pretreated group on day 6.

4.2.3.3. Tissue NO_x levels

In the groups with colitis, a significant elevation in NO_x level was seen in the colonic tissue relative to the controls on day 1. In series 2, the elevation of NO_x was significantly higher in comparison with the control group on day 6. Both PC pretreatment protocols decreased the NO_x elevation, in contrast with the nontreated colitis group on day 6, but the NO_x level in the PC-treated group in Series 2 remained significantly higher than that in the control group on day 1 (Figure 10).
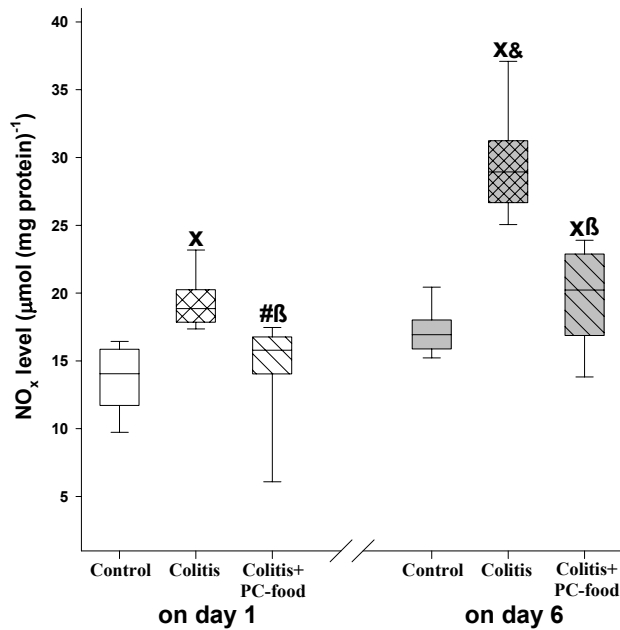

***Figure 10.** Changes in tissue NO_x level on day 1 in the control (white box), colitis (checked white box) and PC-pretreated colitis (striped white box) groups; and on day 6 in the control (empty gray box), colitis (checked gray box) and PC-pretreated colitis (striped gray box) groups. The plots demonstrate the median (horizontal line in the box) and the 25th (lower whisker) and 75th (upper whisker) percentiles. $^x p < 0.05$ between groups and control group on day 1, $^\& p < 0.05$ between groups and control group on day 6, $^\# p < 0.05$ between PC-pretreated groups and colitis group on day 1, $^\beta p<0.05$ between PC-pretreated groups and colitis group on day 6.*

4.2.3.4. In vivo detection of microvessel damage

The colonic microvessels were visualized by FITC-dextran administration and the edema formation was determined by the topical application of acridine orange dye. In the control groups, the network of capillaries exhibited a honeycomb pattern (M = 0; p25 = 0; p75 = 0.275; Figures 11A, D). In Series 1, the confocal microscopic evaluation demonstrated significant tissue damage in acute phases of colitis in contrast with the control groups. The capillary network was disorganized, the honeycomb pattern had disappeared, and fluorescent dye leakage was observed in several areas of the large intestine. A damaged capillary endothelium with edema formation was generally observed (M = 4; p25 = 3.25; p75 = 4; Figure 11B). PC feeding significantly influenced the structural changes in the microvasculature of the inflamed colonic mucosa on day 1 of colitis. The extents of dye

leakage and edema formation were diminished (M=1.5; p25=1; p75=2; Figure 11C).

The tissue damage was also pronounced in the case of subacute colitis in contrast with the control groups. Fluorescent dye leakage with edema formation was seen in the capillary network 6 days after the TNBS enema (M = 2; p25 = 1.625; p75 = 2.375; Figure 11E). By day 6, PC pretreatment prevented the structural changes in the microvasculature of the inflamed colonic mucosa. The histological results indicated decreases in dye leakage and edema (M = 0; p25 = 0; p75 = 0.875; Figure 11F).
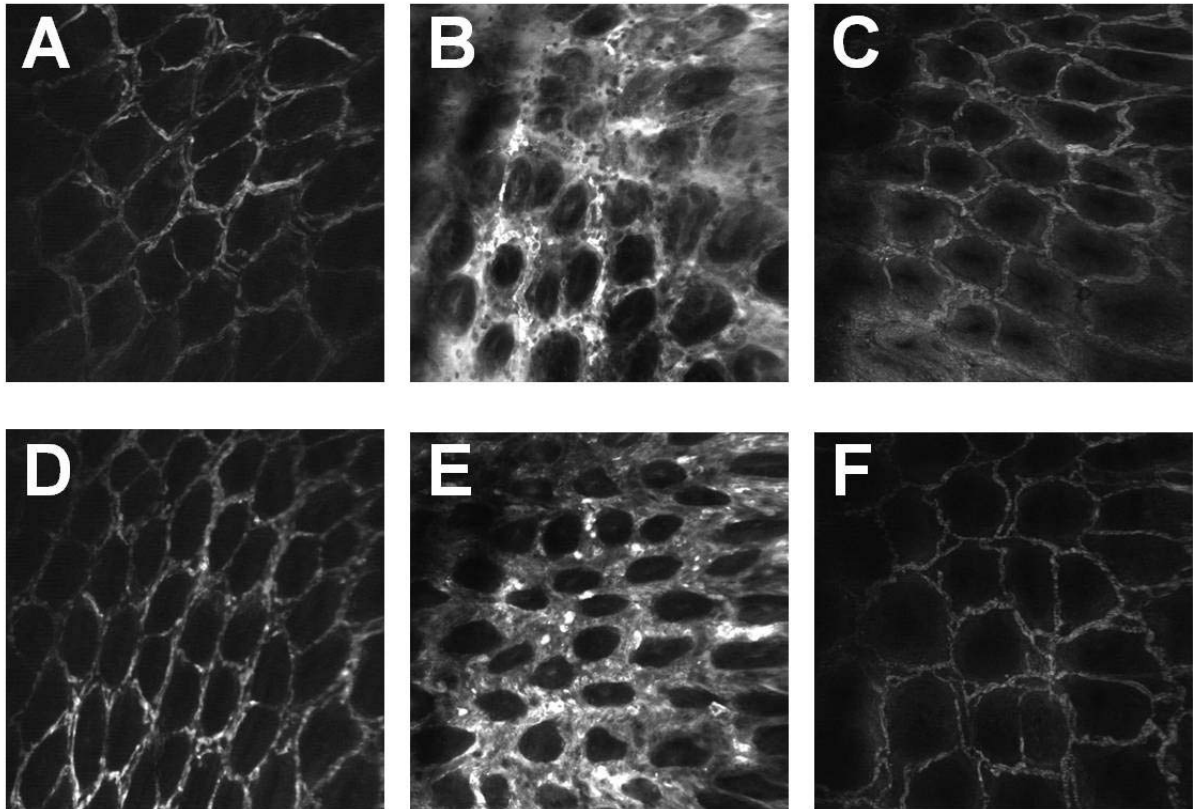
Figure 11. *In vivo histology images of the mucosal surface of the distal rat colon recorded by CLSEM after iv administration of FITC-dextran.* ***A:*** *Normal mucosal vasculature.* ***B:*** *1 day after the TNBS enema, dye leakage from the vessel lumina is observed and the honeycomb pattern of the capillaries has disappeared.* ***C:*** *Moderate dye leakage is observed from the vessel lumina in the PC-pretreated colitis group 1 day after colitis induction.* ***D:*** *Normal mucosal vasculature 6 days after enema of TNBS solvent.* ***E:*** *Six days after colitis induction, dye leakage is observed from the vessel lumina and the normal pattern of the capillaries has disappeared.* ***F:*** *The PC-pretreated group with normal mucosal vasculature 6 days after colitis induction.*

5. DISCUSSION

Mapping of a local microcirculatory dysfunction within the inflamed tissues could be a critical factor to determine the therapeutic approaches in the different inflammatory processes. Therapeutic agents, which improve the function of the microcirculation might be of substantial therapeutic benefit in medical practice. The results of our studies demonstrated significant microcirculatory changes during the acute and subacute phases of TNBS-induced experimental colitis. The therapeutic efficacies of the NMDA receptor antagonist treatments, and pretreatment with oral PC were also evident in our models.

5.1. Evidence of circulatory changes in TNBS-induced colitis

The onset of TNBS-induced colonic inflammation shares many similarities with fulminant episodes of human IBD. This experimental IBD model is characterized by a weight loss (Morris *et al.* 1989) and visceral hyperalgesia (Zhou *et al.* 2008), and is in line with increased plasma levels of the proinflammatory cytokines TNF-α and IL-6 (Hove *et al.* 2001). During the phase of colitis evolution, the barrier function of the mucosal epithelium is rapidly lost (Appleyard *et al.* 2002; Krimsky *et al.* 2003), leading to bacterial translocation and a characteristic hyperdynamic cardiovascular response. The high CO process is regarded as a compensatory change through which the organism strives to accommodate to the emerging septic metabolic changes (Bone 1991).

During IBD, the intramural colonic microcirculation exhibits signs of a microvascular dysfunction, heterogeneous flow with hyperemia (Hatoum *et al.* 2003), vasodilation and venous congestion (Laroux & Grisham 2001). In parallel with these developed macro- and microcirculatory changes, colonic leukocyte recruitment and extravasation have been demonstrated, with significant elevations of NOS activities (Kiss *et al.* 1997; Yue *et al.* 2001). The elevated NO production induces vasodilatation and thereby increases the capillary blood flow in the colonic serosa (Kruschewski *et al.* 2001; Varga *et al.* 2010). The increased leukocyte activation and enhancement of the PMN-endothelial cell interactions are common denominators of these processes (Kruschewski *et al.* 2006).

In our studies, intracolonic TNBS administration induced manifest colitis with a hyperdynamic macrocirculatory reaction, as evidenced by decreased MAP and TPR and elevated CO levels. In the TNBS-treated animals, an increased serosal RBCV was observed in the acute phase. The serosal hyperemia was accompanied by a significant increase in colonic NOS activation. Moreover, an elevation of the MPO activity indicated that the PMNs are still

anchored in the inflamed proximal colon tissue. The subacute phase of colitis is characterized by normal systemic hemodynamics, and moderate serosal hyperemia. The marked leukocyte infiltration in the intestinal tissue was accompanied by biochemical signs of oxidative and nitrosative stress.

The results of *in vivo* CLESM analyses revealed a complete disruption of the capillary network and extended dye leakage. These microcirculatory changes were observed in the acute and subacute phases of TNBS-induced experimental colitis.

5.1.1. Significance of NMDA receptor antagonist therapy in circulatory changes

It has been established that the NMDA receptors play a role in the modulation of the GI function (Liu *et al.* 1997; Giaroni *et al.* 2003). More importantly, other *in vivo* data have shown that the expression of the NMDA receptors increases in peripheral inflammatory reactions (Tan *et al.* 2008) and the receptor upregulation is present on the neurons of the myenteric plexus in TNBS-induced colitis too (Zhou *et al.* 2006).

Treatment with the NMDA receptor antagonist KynA did not significantly influence the overall hemodynamics, but the analog SZR-72 caused a moderate TPR elevation. The difference between the systemic circulatory effects of the examined NMDA antagonists may be linked to the divergent permeabilities of SZR-72 and KynA through the blood-brain barrier. This assumption is supported by the observation that the microinjection of L-glutamate and NMDA into the nucleus tractus solitarius produced a dose-dependent decrease in blood pressure, mesenteric blood flow and iliac vascular resistance. However, previous administration of the NMDA receptor antagonist MK-801 into the same CNS area significantly attenuated this NMDA-induced depressor effect (Tian & Hartle 1994). Unlike KynA (Vécsei *et al.* 1992; Bari *et al.* 2006), SZR-72 readily crosses the blood-brain barrier (Knyihar-Csillik *et al.* 2008) and in this way peripheral hemodynamic reactions may be modulated by CNS effects.

In the acute phase of Study I, the NMDA antagonists reduced the elevated RBCV to normal levels. A further important feature of NMDA receptor antagonist treatment modalities was the parallel influence on the microcirculation, determining distinct elements of the inflammatory response, including the inhibition of local NO synthesis and leukocyte recruitment. The matching effects on the microcirculatory and biochemical responses may be indicative of a connection between the action on local NMDA receptors and the NOS systems. The various NOS isoforms are activated by diverse mechanisms and stimuli, but there is a time-related difference in the activation of the Ca^{2+}-dependent constitutive NOS and

Ca^{2+}-independent iNOS isoforms during this inflammatory process. Both iNOS and eNOS are upregulated in TNBS colitis and reach peak activity after 24 h, subsiding during the ensuing 2 weeks (Petersson *et al.* 2007). The constitutive NOS variants (eNOS or nNOS) permit rapid NO release, but the bulk of the NO is synthesized by the nNOS in the submucous and myenteric plexus of the intestinal wall (Qu *et al.* 1999). iNOS activation is considered a hallmark of inflammation, but it seems that iNOS is not required for the full development of chronic colitis. In iNOS-deficient mice, increases in both macroscopic and microscopic damage have been noted, similarly as in the wild type (McCafferty *et al.* 1999), and iNOS inhibitor treatment does not alter the high rate of perfusion in the colonic microcirculation (Petersson *et al.* 2007). Moreover, it has been demonstrated that the calcium/calmodulin-dependent process (through activation of protein kinase II) significantly inhibits iNOS-specific activity following cytokine induction (Jones *et al.* 2007). Thus, it is reasonable to suggest that the activation of myenteric NMDA receptors is followed by a massive Ca^{2+} influx through the NMDA receptor-ion complex, which stimulates Ca^{2+}-dependent NO synthesis (Liu *et al.* 1997; Furness 2000). The NMDA receptor channel ensures a direct route for Ca^{2+} to the constitutive NOS isoform and XOR, so that the excessive accumulation of glutamate with subsequent activation of the ligand-gated, ion channel NMDA glutamate receptors can lead to stimulation of both constitutive NOS and XOR activities (Furness 2000; Kirchgessner 2001). Accordingly, NMDA receptor inhibition, directly or indirectly linked to NO synthesis reduction, might offer a pathway toward the therapy of intestinal inflammation.

In the subacute phase of Study I, TNBS-induced experimental colitis was associated with significantly increased tissue NO_x levels and tissue nitrotyrosine formation. The pathogenic role of NO-derived species such as peroxynitrite in IBDs is supported by the fact that the intracolonic administration of exogenous peroxynitrite induces severe inflammation, which mimics the features of human ulcerative colitis. Nitrotyrosine has been identified as a marker of cellular damage caused by NO, and it is a specific marker of peroxynitrite. Peroxynitrite produced by the reaction of NO with SOX is highly cytotoxic and is able to induce structural damage (Ko *et al.* 2005; Linden *et al.* 2005). ROS produced in the inflamed mucosa are mainly generated by activated phagocytic leukocytes via NADPH oxidase and the XOR system. The colonic XOR activity was significantly elevated 6 days after TNBS induction, although the level was somewhat lower than in the early phase of colitis (Varga *et al.* 2010). Nevertheless, our results clearly indicated the role of nitrosative stress and the effectiveness of KynA and SZR-72 treatment in decreasing nitrotyrosine formation to the control level.

The second microcirculation-determining factor is the increased leukocyte activation and enhancement of the PMN-endothelial cell interactions in the pathomechanism of IBD. A recent study (Welters *et al.* 2010) disclosed the relationship between NMDA receptor activation and leukocytic cell lines. It has further been demonstrated that NMDA receptors are expressed not only by neurons, but also by a number of non-neuronal cell types, including endothelial cells and immune-competent cells, and this points to the action of a common regulatory mechanism (Boldyrev *et al.* 2004; Hinoi *et al.* 2004; Miglio *et al.* 2005; Reijerkerk *et al.* 2010). Indeed, it has been established that the population of inactive lymphocytes contains only a few cells with NMDA receptors, and expression is induced after appropriate stimuli (Mashkina *et al.* 2010). Moreover, it has been reported that NMDA receptor expression and a normal function are required for activation of the respiratory burst of PMNs (Kim-Park *et al.* 1997). Our results clearly indicated the effectiveness of the examined NMDA receptor antagonist treatments in decreasing leukocyte activation in TNBS-induced experimental colitis.

In fact, the relationship between NMDA receptors and peripheral inflammatory responses has not been completely mapped, but given the role played by NMDA receptor/ leukocyte recruitment signalling during the development and progression of TNBS-induced colitis, direct or indirect reduction of the leukocyte activation may be an appropriate strategy for the simultaneous treatment of the inflammatory changes and intestinal malfunction.

These data additionally indicated that treatment with endogenous or synthetic NMDA receptor antagonists commencing 1 day or 6 days after colitis induction reduces the signs of oxidative and nitrosative stress together with the leukocyte activation and effectively modulates the microcirculatory changes of the process. On the other hand, the single use of NMDA antagonists did not alter the morphological changes in the microvessels and was unable to decrease the small vessel permeability.

5.1.2. Significance of PC therapy in circulatory changes

In Study II, we examined the potentially preventive dietary effects of a PC regimen on the microcirculatory and inflammatory changes in the acute and subacute phases of TNBS-induced colitis. The results demonstrated that a PC-enriched diet reduced the signs of colitis-induced local inflammatory activation as regards the components of nitrosative stress and leukocyte activation, thereby normalizing the colonic mucosal and serosal microcirculation.

Our data from Study II support the results of previous studies that provide evidence of the beneficial effects of PC supplementation in almost every segment of the GI tract

(Lichtenberger 1995; Erős *et al.* 2006; Stremmel *et al.* 2010). In the colon, the protective effects of phospholipids were first outlined after intraluminal application in acetic acid-induced murine colitis (Fabia *et al.* 1992). Polyunsaturated PC mixtures were successfully used in TNBS-provoked colitis (Tatsumi & Lichtenberger 1996) and in a double-blind, randomized, placebo-controlled human study, chronic active IBD patients were treated for 3 months with delayed-release PC without concomitant steroid treatment. 90% of the PC-treated patients reached clinical remission or showed a 50% improvement of their clinical activity (Stremmel *et al.* 2005).

The *in vivo* monitoring of the microcirculation demonstrates that PC-enriched diets reduced the colitis-induced serosal hyperemia and the fluorescent dye leakage from the mucosal capillary network of the colon. These beneficial effects on the microvessel structure and microhemodynamic and biochemical changes were evident both 1 day and also 6 days after the inflammatory challenge.

The serosal microcirculatory hyperemia could be a consequence of the altered synthesis of endothelium-derived mediators, including NO (Hatoum *et al.* 2003), and iNOS-dependent processes. iNOS-derived NO has been implicated in several aspects of the inflammatory cascade in experimental or clinical colitis. We earlier reported that PC treatment inhibited the expression and activity of iNOS isoenzyme *in vivo* (Erős *et al.* 2009) and decreased GI tissue NO_x levels in endotoxemic rats (Tőkés *et al.* 2011), and in the present study PC supplementation significantly decreased the stable end-product of NO in the colon tissue in both phases of colitis.

Moreover, it has been demonstrated that preoperative dietary PC supplementation can indeed either directly or indirectly reduce the ROS-producing activity of the intestinal tissue (Ghyczy *et al.* 2003; Ghyczy *et al.* 2008). Our results show that PC treatment decreased the XOR activity in both examined phases of TNBS-induced experimental colitis. Elevated levels of XOR activity and PMN accumulation are characteristic of GI inflammation, and the inhibition of PMN leukocyte activation and reduction of the tissue concentrations of PMN- or XOR-derived radicals, therefore results in less tissue damage. NO combined with XOR-derived SOX radicals form peroxynitrite, a molecule that is highly damaging to a variety of cells (Beckman *et al.* 1990).

Another explanation is provided if orally administered PC serves as a slow-release blood choline source and the choline component of PC is able to influence the inflammatory process through the cholinergic anti-inflammatory pathway (Tracey *et al.* 2007), including interference with the activation of PMNs. Nevertheless, the mediators formed during the

hydrolysis of PC (*e.g.* betaine and dimethylglycine) may also influence cell-cell interactions in a favorable manner (Ghyczy *et al.* 2003). It was recently found that the multistep extravasation cascade of leukocytes (rolling, adhesion and transmigration) was reduced by PC in the post-ischemic periosteum (Gera *et al.* 2007). Our present results reveal that PC treatment also decreases colitis-induced tissue granulocyte accumulation. An elevated PMN accumulation is characteristic of GI inflammation, and the inhibition of PMN leukocyte activation may result in less tissue damage. In this line, PC metabolites with an alcoholic moiety in the molecule inhibit the ROS-producing activity of PMNs (Ghyczy *et al.* 2003; Ghyczy *et al.* 2008). PC is readily taken up by phagocytic cells and, accordingly, it may accumulate in inflamed tissues (Miranda *et al.* 2008). Other *in vitro* data have shown that dipalmitoyl-PC modulates the inflammatory functions of monocytic cells (Tonks *et al.* 2001) and that a mixture of PC and phosphatidylglycerol inhibits the respiratory burst and SOX generation of human PMNs (Chao *et al.* 1995).

The recent development of a fiberoptic confocal endomicroscope allows potential applications for the noninvasive monitoring of dynamic processes *in vivo* (McLaren *et al.* 2002) and offers a possibility for acquiring more precise *in vivo* data for histological analysis. Cellular and subcellular structures of the colonic epithelium (surface epithelium and crypts), the connective tissue and vasculature could be examined by intravital CLSEM. The CLSEM revealed complete disruption of the capillary network in the early phase, and distortion of the capillary network in the subacute phase of colitis. The *in vivo* and real-time histology data revealed the time-dependent differences in injury of the microvasculature and regeneration of the damaged vessels. PC therapy was successful in decreasing the morphologic damage of the microvessels and thereby decreased the vascular permeability.

In conclusion, we have demonstrated that PC feeding effectively modulates the inflammatory processes and normalizes the changes in the microcirculation 1 day and 6 days after colitis induction. A direct beneficial effect of dietary PC supplementation may be the prevention of the injury of the microvessel structure, and the resulting prevention of the elevation of the vascular permeability.

6. SUMMARY OF NEW FINDINGS

1. The results showed that intravital microcirculatory evaluations with OPS can be used for visualization and quantitative assessment of the microcirculation at the bedside in inflammatory conditions of the GI tract. Similarly, CLSEM can be used to determine the functional and morphological changes of the microvessels and to investigate the microvascular permeability in *real time*. These intravital imaging techniques may replace the conventional histological methods, because high-resolution histological images could be taken without physical disruption of the observed tissues.

2. Our findings indicate that both microcirculatory examination techniques can be effectively used to monitor the microvascular function. However, it is important to note that neither of them can be replaced by the other; rather, they have a complementary role in microcirculatory examinations.

3. We have successfully set up a new scoring system for the evaluation of microvessel injury in the records taken by CLSEM. We have demonstrated for the first time that this scoring system can be used in *in vivo* histological investigations of inflammatory conditions of the GI tract.

4. Blockade of the enteric NMDA receptors provides a therapeutic possibility by targeting the local inflammatory changes and microcirculatory injury in the early and later phases of acute colitis. Although single treatments with the NMDA receptor antagonist KynA or SZR-72 were not capable of influencing the microvascular damage in TNBS colitis, both NMDA receptor antagonists have the potential to normalize the elevated serosal RBCV. These effects are associated with decreasing PMN leukocyte accumulation and NO production in the proximal colon 1 and 6 days after TNBS administration.

5. PC pretreatment proved to be effective in preventing the deterioration of the microcirculation and injuries of the microvessels in the intestinal wall in both phases of experimental TNBS colitis. The drug administration decreased the elevated PMN leukocyte accumulation, the XOR activity and NO production in the proximal colon 1 and 6 days after TNBS administration.

7. REFERENCE LIST

1. Appleyard, C. B., Alvarez, A. & Percy, W. H. (2002). Temporal changes in colonic vascular architecture and inflammatory mediator levels in animal models of colitis. *Dig.Dis.Sci.,* 47, 2007-2014.

2. Bari, F., Nagy, K., Guidetti, P., Schwarcz, R., Busija, D. W. & Domoki, F. (2006). Kynurenic acid attenuates NMDA-induced pial arteriolar dilation in newborn pigs. *Brain Res.,* 1069, 39-46.

3. Beckman, J. S. (1990). Ischaemic injury mediator. *Nature,* 345, 27-28.

4. Beckman, J. S., Beckman, T. W., Chen, J., Marshall, P. A. & Freeman, B. A. (1990). Apparent hydroxyl radical production by peroxynitrite: implications for endothelial injury from nitric oxide and superoxide. *Proc.Natl.Acad.Sci.U.S.A,* 87, 1620-1624.

5. Beckman, J. S., Parks, D. A., Pearson, J. D., Marshall, P. A. & Freeman, B. A. (1989). A sensitive fluorometric assay for measuring xanthine dehydrogenase and oxidase in tissues. *Free Radic.Biol.Med.,* 6, 607-615.

6. Blusztajn, J. K. & Wurtman, R. J. (1983). Choline and cholinergic neurons. *Science,* 221, 614-620.

7. Boldyrev, A. A., Kazey, V. I., Leinsoo, T. A., Mashkina, A. P., Tyulina, O. V., Johnson, P., Tuneva, J. O., Chittur, S. & Carpenter, D. O. (2004). Rodent lymphocytes express functionally active glutamate receptors. *Biochem.Biophys.Res.Commun.,* 324, 133-139.

8. Bone, R. C. (1991). The pathogenesis of sepsis. *Ann.Intern.Med.,* 115, 457-469.

9. Braus, N. A. & Elliott, D. E. (2009). Advances in the pathogenesis and treatment of IBD. *Clin.Immunol.,* 132, 1-9.

10. Choi, D. W., Koh, J. Y. & Peters, S. (1988). Pharmacology of glutamate neurotoxicity in cortical cell culture: attenuation by NMDA antagonists. *J.Neurosci.,* 8, 185-196.

11. Christmas, D. M., Badawy, A. A., Hince, D., Davies, S. J., Probert, C., Creed, T., Smithson, J., Afzal, M., Nutt, D. J. & Potokar, J. P. (2010). Increased serum free tryptophan in patients with diarrhea-predominant irritable bowel syndrome. *Nutr.Res.,* 30, 678-688.

12. Cleland, L. G., Shandling, M., Percy, J. S. & Poznansky, M. J. (1979). Liposomes: a new approach to gold therapy? *J.Rheumatol.Suppl,* 5, 154-163.

13. De Backer, D., Ospina-Tascon, G., Salgado, D., Favory, R., Creteur, J. & Vincent, J. L. (2010). Monitoring the microcirculation in the critically ill patient: current methods and future approaches. *Intensive Care Med.,* 36, 1813-1825.

14. Duran, W. N., Breslin, J. W. & Sanchez, F. A. (2010). The NO cascade, eNOS location, and microvascular permeability. *Cardiovasc.Res.,* 87, 254-261.

15. el-Hariri, L. M., Marriott, C. & Martin, G. P. (1992). The mitigating effects of

phosphatidylcholines on bile salt- and lysophosphatidylcholine-induced membrane damage. *J.Pharm.Pharmacol.,* 44, 651-654.

16. Erős, G., Ibrahim, S., Siebert, N., Boros, M. & Vollmar, B. (2009). Oral phosphatidylcholine pretreatment alleviates the signs of experimental rheumatoid arthritis. *Arthritis Res.Ther.,* 11, R43.

17. Erős, G., Kaszaki, J., Czóbel, M. & Boros, M. (2006). Systemic phosphatidylcholine pretreatment protects canine esophageal mucosa during acute experimental biliary reflux. *World J.Gastroenterol.,* 12, 271-279.

18. Fabia, R., Ar'Rajab, A., Willen, R., Andersson, R., Ahren, B., Larsson, K. & Bengmark, S. (1992). Effects of phosphatidylcholine and phosphatidylinositol on acetic-acid-induced colitis in the rat. *Digestion,* 53, 35-44.

19. Faden, A. I., Demediuk, P., Panter, S. S. & Vink, R. (1989). The role of excitatory amino acids and NMDA receptors in traumatic brain injury. *Science,* 244, 798-800.

20. Foitzik, T., Kruschewski, M., Kroesen, A. J., Hotz, H. G., Eibl, G. & Buhr, H. J. (1999). Does glutamine reduce bacterial translocation? A study in two animal models with impaired gut barrier. *Int.J.Colorectal Dis.,* 14, 143-149.

21. Forrest, C. M., Youd, P., Kennedy, A., Gould, S. R., Darlington, L. G. & Stone, T. W. (2002). Purine, kynurenine, neopterin and lipid peroxidation levels in inflammatory bowel disease. *J.Biomed.Sci.,* 9, 436-442.

22. Fülöp, F., Szatmári, I., Vámos, E., Zádori, D., Toldi, J. & Vécsei, L. (2009). Syntheses, transformations and pharmaceutical applications of kynurenic acid derivatives. *Curr.Med.Chem.,* 16, 4828-4842.

23. Furness, J. B. (2000). Types of neurons in the enteric nervous system. *J.Auton.Nerv.Syst.,* 81, 87-96.

24. Gera, L., Varga, R., Török, L., Kaszaki, J., Szabó, A., Nagy, K. & Boros, M. (2007). Beneficial effects of phosphatidylcholine during hindlimb reperfusion. *J.Surg.Res.,* 139, 45-50.

25. Ghyczy, M., Torday, C. & Boros, M. (2003). Simultaneous generation of methane, carbon dioxide, and carbon monoxide from choline and ascorbic acid: a defensive mechanism against reductive stress? *FASEB J.,* 17, 1124-1126.

26. Ghyczy, M., Torday, C., Kaszaki, J., Szabó, A., Czóbel, M. & Boros, M. (2008). Oral phosphatidylcholine pretreatment decreases ischemia-reperfusion-induced methane generation and the inflammatory response in the small intestine. *Shock,* 30, 596-602.

27. Giaroni, C., Zanetti, E., Chiaravalli, A. M., Albarello, L., Dominioni, L., Capella, C., Lecchini, S. & Frigo, G. (2003). Evidence for a glutamatergic modulation of the cholinergic function in the human enteric nervous system via NMDA receptors. *Eur.J.Pharmacol.,* 476, 63-69.

28. Granger, D. N. (1988). Role of xanthine oxidase and granulocytes in ischemia-reperfusion injury. *Am.J.Physiol,* 255, H1269-H1275.

29. Granger, D. N. (1999). Ischemia-reperfusion: mechanisms of microvascular dysfunction and the influence of risk factors for cardiovascular disease. *Microcirculation.,* 6, 167-178.

30. Granger, D. N. & Kubes, P. (1994). The microcirculation and inflammation: modulation of leukocyte-endothelial cell adhesion. *J.Leukoc.Biol.,* 55, 662-675.

31. Granger, H. J., Schelling, M. E., Lewis, R. E., Zawieja, D. C. & Meininger, C. J. (1988). Physiology and pathobiology of the microcirculation. *Am.J.Otolaryngol.,* 9, 264-277.

32. Groner, W., Winkelman, J. W., Harris, A. G., Ince, C., Bouma, G. J., Messmer, K. & Nadeau, R. G. (1999). Orthogonal polarization spectral imaging: a new method for study of the microcirculation. *Nat.Med.,* 5, 1209-1212.

33. Gross, V., Andus, T., Leser, H. G., Roth, M. & Scholmerich, J. (1991). Inflammatory mediators in chronic inflammatory bowel diseases. *Klin.Wochenschr.,* 69, 981-987.

34. Guslandi, M. (1986). Mucosal blood flow and gastric protection--effect of neurohormonal and pharmacological agents. *Int.J.Clin.Pharmacol.Ther.Toxicol.,* 24, 143-147.

35. Hasibeder, W. (2010). Gastrointestinal microcirculation: still a mystery? *Br.J.Anaesth.,* 105, 393-396.

36. Hatoum, O. A., Binion, D. G., Otterson, M. F. & Gutterman, D. D. (2003). Acquired microvascular dysfunction in inflammatory bowel disease: Loss of nitric oxide-mediated vasodilation. *Gastroenterology,* 125, 58-69.

37. Hinoi, E., Takarada, T. & Yoneda, Y. (2004). Glutamate signaling system in bone. *J.Pharmacol.Sci.,* 94, 215-220.

38. Hwang, J. M. & Varma, M. G. (2008). Surgery for inflammatory bowel disease. *World J.Gastroenterol.,* 14, 2678-2690.

39. Ince, C. (2005). The microcirculation is the motor of sepsis. *Crit Care,* 9 Suppl 4, S13-S19.

40. Johnson, P. C. & Henrich, H. A. (1975). Metabolic and myogenic factors in local regulation of the microcirculation. *Fed.Proc.,* 34, 2020-2024.

41. Jones, R. J., Jourd'heuil, D., Salerno, J. C., Smith, S. M. & Singer, H. A. (2007). iNOS regulation by calcium/calmodulin-dependent protein kinase II in vascular smooth muscle. *Am.J.Physiol Heart Circ.Physiol,* 292, H2634-H2642.

42. Kessler, M., Terramani, T., Lynch, G. & Baudry, M. (1989). A glycine site associated with N-methyl-D-aspartic acid receptors: characterization and identification of a new class of antagonists. *J.Neurochem.,* 52, 1319-1328.

43. Kiesslich, R., Goetz, M., Angus, E. M., Hu, Q., Guan, Y., Potten, C., Allen, T., Neurath, M. F., Shroyer, N. F., Montrose, M. H. & Watson, A. J. (2007). Identification of epithelial gaps in human small and large intestine by confocal

endomicroscopy. *Gastroenterology,* 133, 1769-1778.

44. Kim-Park, W. K., Moore, M. A., Hakki, Z. W. & Kowolik, M. J. (1997). Activation of the neutrophil respiratory burst requires both intracellular and extracellular calcium. *Ann.N.Y.Acad.Sci.,* 832, 394-404.

45. Kirchgessner, A. L. (2001). Glutamate in the enteric nervous system. *Curr.Opin.Pharmacol.,* 1, 591-596.

46. Kiss, J., Lamarque, D., Delchier, J. C. & Whittle, B. J. (1997). Time-dependent actions of nitric oxide synthase inhibition on colonic inflammation induced by trinitrobenzene sulphonic acid in rats. *Eur.J.Pharmacol.,* 336, 219-224.

47. Klivényi, P., Toldi, J. & Vécsei, L. (2004). Kynurenines in neurodegenerative disorders: therapeutic consideration. *Adv.Exp.Med.Biol.,* 541, 169-183.

48. Knyihar-Csillik, E., Mihaly, A., Krisztin-Péva, B., Robotka, H., Szatmari, I., Fülöp, F., Toldi, J., Csillik, B. & Vécsei, L. (2008). The kynurenate analog SZR-72 prevents the nitroglycerol-induced increase of c-fos immunoreactivity in the rat caudal trigeminal nucleus: comparative studies of the effects of SZR-72 and kynurenic acid. *Neurosci.Res.,* 61, 429-432.

49. Ko, J. K., Lam, F. Y. & Cheung, A. P. (2005). Amelioration of experimental colitis by Astragalus membranaceus through anti-oxidation and inhibition of adhesion molecule synthesis. *World J.Gastroenterol.,* 11, 5787-5794.

50. Krimsky, M., Yedgar, S., Aptekar, L., Schwob, O., Goshen, G., Gruzman, A., Sasson, S. & Ligumsky, M. (2003). Amelioration of TNBS-induced colon inflammation in rats by phospholipase A2 inhibitor. *Am.J.Physiol Gastrointest.Liver Physiol,* 285, G586-G592.

51. Kruschewski, M., Anderson, T., Buhr, H. J. & Loddenkemper, C. (2006). Selective COX-2 inhibition reduces leukocyte sticking and improves the microcirculation in TNBS colitis. *Dig.Dis.Sci.,* 51, 662-670.

52. Kruschewski, M., Foitzik, T., Perez-Canto, A., Hubotter, A. & Buhr, H. J. (2001). Changes of colonic mucosal microcirculation and histology in two colitis models: an experimental study using intravital microscopy and a new histological scoring system. *Dig.Dis.Sci.,* 46, 2336-2343.

53. Kuebler, W. M., Abels, C., Schuerer, L. & Goetz, A. E. (1996). Measurement of neutrophil content in brain and lung tissue by a modified myeloperoxidase assay. *Int.J.Microcirc.Clin.Exp.,* 16, 89-97.

54. Laroux, F. S. & Grisham, M. B. (2001). Immunological basis of inflammatory bowel disease: role of the microcirculation. *Microcirculation.,* 8, 283-301.

55. Lee, H. C., Fellenz-Maloney, M. P., Liscovitch, M. & Blusztajn, J. K. (1993). Phospholipase D-catalyzed hydrolysis of phosphatidylcholine provides the choline precursor for acetylcholine synthesis in a human neuronal cell line. *Proc.Natl.Acad.Sci.U.S.A,* 90, 10086-10090.

56. Lichtenberger, L. M. (1995). The hydrophobic barrier properties of gastrointestinal mucus. *Annu.Rev.Physiol,* 57, 565-583.

57. Linden, D. R., Couvrette, J. M., Ciolino, A., McQuoid, C., Blaszyk, H., Sharkey, K. A. & Mawe, G. M. (2005). Indiscriminate loss of myenteric neurones in the TNBS-inflamed guinea-pig distal colon. *Neurogastroenterol.Motil.,* 17, 751-760.

58. Lindert, J., Werner, J., Redlin, M., Kuppe, H., Habazettl, H. & Pries, A. R. (2002). OPS imaging of human microcirculation: a short technical report. *J.Vasc.Res.,* 39, 368-372.

59. Liu, M. T., Rothstein, J. D., Gershon, M. D. & Kirchgessner, A. L. (1997). Glutamatergic enteric neurons. *J.Neurosci.,* 17, 4764-4784.

60. Masaki, T. (1989). The discovery, the present state, and the future prospects of endothelin. *J.Cardiovasc.Pharmacol.,* 13 Suppl 5, S1-S4.

61. Mashkina, A. P., Cizkova, D., Vanicky, I. & Boldyrev, A. A. (2010). NMDA receptors are expressed in lymphocytes activated both in vitro and in vivo. *Cell Mol.Neurobiol.,* 30, 901-907.

62. McCafferty, D. M., Miampamba, M., Sihota, E., Sharkey, K. A. & Kubes, P. (1999). Role of inducible nitric oxide synthase in trinitrobenzene sulphonic acid induced colitis in mice. *Gut,* 45, 864-873.

63. McLaren, W., Anikijenko, P., Barkla, D., Delaney, T. P. & King, R. (2001). In vivo detection of experimental ulcerative colitis in rats using fiberoptic confocal imaging (FOCI). *Dig.Dis.Sci.,* 46, 2263-2276.

64. Miglio, G., Varsaldi, F. & Lombardi, G. (2005). Human T lymphocytes express N-methyl-D-aspartate receptors functionally active in controlling T cell activation. *Biochem.Biophys.Res.Commun.,* 338, 1875-1883.

65. Moncada, S. (1999). Nitric oxide: discovery and impact on clinical medicine. *J.R.Soc.Med.,* 92, 164-169.

66. Moncada, S. & Higgs, E. A. (1991). Endogenous nitric oxide: physiology, pathology and clinical relevance. *Eur.J.Clin.Invest,* 21, 361-374.

67. Moncada, S., Palmer, R. M. & Higgs, E. A. (1991). Nitric oxide: physiology, pathophysiology, and pharmacology. *Pharmacol.Rev.,* 43, 109-142.

68. Monje, M. L., Toda, H. & Palmer, T. D. (2003). Inflammatory blockade restores adult hippocampal neurogenesis. *Science,* 302, 1760-1765.

69. Morris, G. P., Beck, P. L., Herridge, M. S., Depew, W. T., Szewczuk, M. R. & Wallace, J. L. (1989). Hapten-induced model of chronic inflammation and ulceration in the rat colon. *Gastroenterology,* 96, 795-803.

70. Moshage, H., Kok, B., Huizenga, J. R. & Jansen, P. L. (1995). Nitrite and nitrate determinations in plasma: a critical evaluation. *Clin.Chem.,* 41, 892-896.

71. Neurath, M. F., Fuss, I., Pasparakis, M., Alexopoulou, L., Haralambous, S., Meyer Zum Buschenfelde, K. H., Strober, W. & Kollias, G. (1997). Predominant pathogenic role of tumor necrosis factor in experimental colitis in mice. *Eur.J.Immunol.,* 27, 1743-1750.

72. Niederau, C., Backmerhoff, F., Schumacher, B. & Niederau, C. (1997). Inflammatory mediators and acute phase proteins in patients with Crohn's disease and ulcerative colitis. *Hepatogastroenterology,* 44, 90-107.

73. Palmer, R. M., Ferrige, A. G. & Moncada, S. (1987). Nitric oxide release accounts for the biological activity of endothelium-derived relaxing factor. *Nature,* 327, 524-526.

74. Perrier, C. & Rutgeerts, P. (2012). New drug therapies on the horizon for IBD. *Dig.Dis.,* 30 Suppl 1, 100-105.

75. Petersson, J., Schreiber, O., Steege, A., Patzak, A., Hellsten, A., Phillipson, M. & Holm, L. (2007). eNOS involved in colitis-induced mucosal blood flow increase. *Am.J.Physiol Gastrointest.Liver Physiol,* 293, G1281-G1287.

76. Qu, X. W., Wang, H., Rozenfeld, R. A., Huang, W. & Hsueh, W. (1999). Type I nitric oxide synthase (NOS) is the predominant NOS in rat small intestine. Regulation by platelet-activating factor. *Biochim.Biophys.Acta,* 1451, 211-217.

77. Radi, R., Beckman, J. S., Bush, K. M. & Freeman, B. A. (1991). Peroxynitrite oxidation of sulfhydryls. The cytotoxic potential of superoxide and nitric oxide. *J.Biol.Chem.,* 266, 4244-4250.

78. Reijerkerk, A., Kooij, G., van der Pol, S. M., Leyen, T., Lakeman, K., van Het, H. B., Vivien, D. & de Vries, H. E. (2010). The NR1 subunit of NMDA receptor regulates monocyte transmigration through the brain endothelial cell barrier. *J.Neurochem.,* 113, 447-453.

79. Rutgeerts, P., Van, A. G. & Vermeire, S. (2004). Optimizing anti-TNF treatment in inflammatory bowel disease. *Gastroenterology,* 126, 1593-1610.

80. Simon, R. P., Young, R. S., Stout, S. & Cheng, J. (1986). Inhibition of excitatory neurotransmission with kynurenate reduces brain edema in neonatal anoxia. *Neurosci.Lett.,* 71, 361-364.

81. Sinsky, M. & Donnerer, J. (1998). Evidence for a neurotransmitter role of glutamate in guinea pig myenteric plexus neurons. *Neurosci.Lett.,* 258, 109-112.

82. Stone, T. W. (1993). Subtypes of NMDA receptors. *Gen.Pharmacol.,* 24, 825-832.

83. Stremmel, W., Hanemann, A., Ehehalt, R., Karner, M. & Braun, A. (2010). Phosphatidylcholine (lecithin) and the mucus layer: Evidence of therapeutic efficacy in ulcerative colitis? *Dig.Dis.,* 28, 490-496.

84. Stremmel, W., Merle, U., Zahn, A., Autschbach, F., Hinz, U. & Ehehalt, R. (2005). Retarded release phosphatidylcholine benefits patients with chronic active ulcerative colitis. *Gut,* 54, 966-971.

85. Szabó, C., Mitchell, J. A., Thiemermann, C. & Vane, J. R. (1993). Nitric oxide-mediated hyporeactivity to noradrenaline precedes the induction of nitric oxide synthase in endotoxin shock. *Br.J.Pharmacol.,* 108, 786-792.

86. Tatsumi, Y. & Lichtenberger, L. M. (1996a). Molecular association of trinitrobenzenesulfonic acid and surface phospholipids in the development of colitis in rats. *Gastroenterology,* 110, 780-789.

87. Ten, H. T., Corbaz, A., Amitai, H., Aloni, S., Belzer, I., Graber, P., Drillenburg, P., Van Deventer, S. J., Chvatchko, Y. & Te Velde, A. A. (2001). Blockade of endogenous IL-18 ameliorates TNBS-induced colitis by decreasing local TNF-alpha production in mice. *Gastroenterology,* 121, 1372-1379.

88. Tian, B. & Hartle, D. K. (1994). Cardiovascular effects of NMDA and MK-801 infusion at area postrema and mNTS in rat. *Pharmacol.Biochem.Behav.,* 49, 489-495.

89. Tőkés, T., Erős, G., Bebes, A., Hartmann, P., Varszegi, S., Varga, G., Kaszaki, J., Gulya, K., Ghyczy, M. & Boros, M. (2011). Protective effects of a phosphatidylcholine-enriched diet in lipopolysaccharide-induced experimental neuroinflammation in the rat. *Shock,* 36, 458-465.

90. Torres, M. I., Lopez-Casado, M. A., Lorite, P. & Rios, A. (2007). Tryptophan metabolism and indoleamine 2,3-dioxygenase expression in coeliac disease. *Clin.Exp.Immunol.,* 148, 419-424.

91. Treede, I., Braun, A., Sparla, R., Kuhnel, M., Giese, T., Turner, J. R., Anes, E., Kulaksiz, H., Fullekrug, J., Stremmel, W., Griffiths, G. & Ehehalt, R. (2007). Anti-inflammatory effects of phosphatidylcholine. *J.Biol.Chem.,* 282, 27155-27164.

92. Ulus, I. H., Wurtman, R. J., Mauron, C. & Blusztajn, J. K. (1989). Choline increases acetylcholine release and protects against the stimulation-induced decrease in phosphatide levels within membranes of rat corpus striatum. *Brain Res.,* 484, 217-227.

93. Varga, G., Érces, D., Fazekas, B., Fülöp, M., Kovacs, T., Kaszaki, J., Fülöp, F., Vécsei, L. & Boros, M. (2010). N-Methyl-D-aspartate receptor antagonism decreases motility and inflammatory activation in the early phase of acute experimental colitis in the rat. *Neurogastroenterol.Motil.,* 22, 217-25, e68.

94. Vécsei, L., Miller, J., MacGarvey, U. & Beal, M. F. (1992). Kynurenine and probenecid inhibit pentylenetetrazol- and NMDLA-induced seizures and increase kynurenic acid concentrations in the brain. *Brain Res.Bull.,* 28, 233-238.

95. Welters, I. D., Hafer, G., Menzebach, A., Muhling, J., Neuhauser, C., Browning, P. & Goumon, Y. (2010). Ketamine inhibits transcription factors activator protein 1 and nuclear factor-kappaB, interleukin-8 production, as well as CD11b and CD16 expression: studies in human leukocytes and leukocytic cell lines. *Anesth.Analg.,* 110, 934-941.

96. Wiley, J. W., Lu, Y. X. & Owyang, C. (1991). Evidence for a glutamatergic neural pathway in the myenteric plexus. *Am.J.Physiol,* 261, G693-G700.

97. Yue, G., Lai, P. S., Yin, K., Sun, F. F., Nagele, R. G., Liu, X., Linask, K. K., Wang,

C., Lin, K. T. & Wong, P. Y. (2001). Colon epithelial cell death in 2,4,6-trinitrobenzenesulfonic acid-induced colitis is associated with increased inducible nitric-oxide synthase expression and peroxynitrite production. *J.Pharmacol.Exp.Ther.,* 297, 915-925.

98. Zhou, Q., Caudle, R. M., Price, D. D., Del Valle-Pinero, A. Y. & Verne, G. N. (2006). Selective up-regulation of NMDA-NR1 receptor expression in myenteric plexus after TNBS induced colitis in rats. *Mol.Pain,* 2, 3.

99. Zhou, Q., Price, D. D., Caudle, R. M. & Verne, G. N. (2008). Visceral and somatic hypersensitivity in TNBS-induced colitis in rats. *Dig.Dis.Sci.,* 53, 429-435.

100. Zorov, D. B., Juhaszova, M. & Sollott, S. J. (2006). Mitochondrial ROS-induced ROS release: an update and review. *Biochim.Biophys.Acta,* 1757, 509-517.

8. ACKNOWLEDGMENTS

I would like to express my gratitude to Professor Mihály Boros, head of the Institute of Surgical Research, for his scientific guidance. I appreciate the encouragement and support he has given me through the years during which I had the possibility to work in his department.

I owe especiall thanks to my supervisor, Dr. József Kaszaki, for his personal guidance and for introducing me to experimental surgery. Without his continuous support, never-failing interest and optimistic attitude to the scientific problems, this PhD study could hardly have been completed.

I am grateful to Dr. Dániel Érces for his valuable help in supporting my experimental work.

I am indebted to Dr. Andrea Szabó, who helped me to learn the basic experimental skills.

My special thanks are due to all the technical staff at the Institute of Surgical Research for their skillful assistance.

9. ANNEX